UV-Induced DNA Repair Mechanisms and Their Effects on Mutagenesis and Culturability in *Escherichia coli*

Sreyashi Ghosh, and Mehmet A. Orman*
William A. Brookshire Department of Chemical and Biomolecular Engineering, University of Houston, Houston, TX, USA

*Correspondence to: S222 Engineering Bldg 1, 4226 Martin Luther King Boulevard, Houston, TX 77204-4004, Phone: 713-743-6785, Email: morman@central.uh.edu

Abstract

Mutagenic processes drive evolutionary progress, with ultraviolet (UV) radiation significantly affecting evolution. Despite extensive research on SOS response-mediated mutagenesis, UV-induced repair mechanisms remain complex, and their effects on cell survival and mutagenesis are not fully understood. We previously observed a near-perfect correlation between RecA-mediated SOS response and mutation levels in *Escherichia coli* following UV treatment. However, prolonged UV exposure caused transient non-culturability and impaired SOS-mediated mutagenesis. Using fluorescent reporters, flow cytometry, promoter-reporter assays, single-gene deletions, knockouts, and clonogenic assays, we found that excessive UV exposure disrupts cellular translation, reducing SOS gene expression, albeit with minimal impact on membrane permeability or reactive oxygen species levels. While our findings underline the abundance of repair mechanisms in *E. coli* cells, enabling them to compensate when specific genes are disrupted, they also highlighted the differential impacts of gene deletions on mutagenesis versus culturability, leading to three major outcomes: (i) Disruption of proteins involved in DNA polymerase for trans-lesion synthesis (UmuC and UmuD) or Holliday junction resolution (RuvC) results in significantly decreased mutagenesis levels while maintaining a transient non-culturability pattern after UV exposure. (ii) Disruption of proteins involved in homologous recombination (RecA and RecB) and nucleotide excision repair (UvrA) leads to both significantly reduced mutagenesis and a more severe transient non-culturability pattern after UV exposure, making these cells more sensitive to UV. (iii) Disruption of DNA Helicase II (UvrD), which functions in mismatch repair, does not affect mutagenesis levels from UV radiation but results in a very pronounced transient non-culturability pattern following UV exposure. Overall, our results further advance our understanding of bacterial adaptation mechanisms and the role of DNA repair pathways in shaping mutagenesis.

Author Summary

Ultraviolet (UV) radiation has been a significant force in driving genetic variation and adaptation throughout billions of years of evolution. By directly damaging DNA and triggering repair mechanisms, UV radiation is a powerful tool for studying mutagenesis. This study aims to provide new insights into the complex processes behind bacterial mutagenesis, a critical topic in microbiology and public health. Although the connection between the SOS response and DNA repair in UV-treated cells is well known, two key phenomena — UV-induced bacterial cell dormancy and mutagenesis — remain poorly understood. Our findings reveal a highly unusual,

SOS response-dependent transient non-culturability in *Escherichia coli* cells following prolonged UV exposure. However, the downstream mechanisms of this phenomenon and its links to mutagenesis remain unclear. This study seeks to thoroughly investigate these phenomena, offering new insights into their underlying molecular processes.

Introduction

Mutagenic processes are key to evolutionary progress [1–3], as they generate genetic diversity. This is essential for organisms to adapt to and endure in dynamic settings that are continuously changing. Understanding the mechanisms underlying mutagenesis helps us better comprehend the evolutionary forces shaping organisms [4,5]. This knowledge also aids in developing more potent and effective medical treatments to combat many diseases, given that pathogenic microorganisms and tumorigenic cells develop resistance through mutagenesis[6–9].

Ultraviolet (UV) radiation has continually shaped the trajectory of evolution over billions of years, from contributing to the origins of life to driving genetic variation and adaptation[10,11]. This is because UV radiation directly damages DNA and induces certain repair mechanisms that are highly mutagenic[12–15]. The UV light spectrum, ranging from 100 to 400 nanometers (nm), can be categorized into four groups: UV-A (315-400 nm), UV-B (280-315 nm), UV-C (100-280 nm), and vacuum-UV (100-200 nm)[16]. UV-C is more readily absorbed by nucleic acids compared to UV-B and UV-A[17]. When bacteria are exposed to UV radiation, [6,7] including UV-C, UV-B, and UV-A, it triggers the formation of pyrimidine dimers and other DNA lesions that disrupt the normal structure and function of DNA molecules[18,19]. These UV lesions are removed by various effective bacterial systems, such as the photoreactivation repair system, (i.e. dimer monomerization under visible light by photolyase enzymes[20]), base excision repair (BER) (removal of cyclobutane-thymine dimers using DNA glycosylases and AP endonucleases)[21], and the primary pathway for removal of bulky DNA lesions, i.e. the nucleotide excision repair (NER) (for rapid repair of photo-lesions using the *uvr* genes, *polA* and ligase enzyme) [22]. However, an excessive amount of dimers that cannot be removed by the repair systems can accumulate and interfere with the cellular replication process, resulting in the formation of "secondary" lesions in the form of ssDNA fragments[23]. Therefore, to deal with this severe DNA damage, a post-replication damage repair mechanism known as the bacterial SOS response pathway is induced, preventing premature cell division [12,24,25] and providing cells with sufficient time to repair the damaged DNA[14,26–28]. This SOS response in bacteria is controlled by the multifunctional RecA protein, a key component that cleaves the transcriptional repressor LexA[29–31]. This cleavage initiates the expression of more than 40 SOS genes. RecA, involved in the recombination repair of ssDNA gaps[32], helps provide an error-free damage removal route. However, excessive DNA damage leads to the induction of the mutagenic phase of the SOS response, mediated by bacterial DNA polymerase enzymes, including Pol V [33,34] , which is encoded by the *umuD* and *umuC* genes [35]. Pol V can bypass template lesions during DNA replication through a process known as translesion DNA synthesis (TLS) [36]. Two additional TLS DNA polymerases, Pol II (encoded by *polB*) and Pol IV (encoded by *dinB*), facilitate replication past blocking lesions, albeit at the cost of introducing mutations. Another DNA damage repair strategy is the mismatch repair (MMR) pathway [37], which recognizes base-base mismatches and insertion/deletion loops, including those introduced by DNA polymerases and as part of TLS during the SOS response. However, with increased mutagenic stress, the efficiency of MMR decreases, as observed in the case of fluoroquinolone treatment [38].

UV radiation can serve as a valuable experimental tool for investigating mutagenesis because it induces a wide range of mutations without an apparent sequence preference[39,40]. Additionally, UV

radiation is of great interest to scientists for its applications in biotechnology, particularly in directed evolutionary strategies to engineer proteins or organisms[41,42] . Moreover, there is growing interest in using UV radiation as a disinfectant, including for sterilizing air, equipment, and surfaces; reducing the transmission of airborne diseases; and even treating wound infections[43,44]. Despite their increased applications in clinical settings, we believe that two phenomena— UV-induced bacterial cell dormancy and mutagenesis— need to be fully understood. Bacterial cells are highly heterogeneous, and they can enter a growth-arrested state through stochastic mechanisms or environmental factors[45], including UV treatment, which can make these cells highly tolerant. Also, the SOS-response-mediated cell dormancy not only promotes cell survival but also sustains mutagenic processes, as dormant cells may still harbor DNA damage[46,47]. Additionally, UV radiation itself is highly mutagenic; it can accelerate the emergence of more resilient mutants, which could pose a serious threat to public health.

UV-induced repair mechanisms are highly complex as UV can damage many cellular components, including DNA, RNA, lipids, and proteins[48,49]. Although the role of the SOS response in mutagenesis has been extensively studied (refer to the following review articles[12,26,28] for more details), our understanding of the downstream repair mechanisms and their contributions to cell survival, culturability, and mutagenesis remains limited. In our recent study[50], we observed a significant correlation between the RecA-mediated SOS response and mutation levels. Additionally, prolonged UV exposure was found to impair SOS-mediated mutagenesis and induce a transient non-culturability state [50], which may represent a potential survival strategy for cells to evade UV-induced mutagenesis. However, the underlying mechanisms remain unclear. Our current study aims to investigate these complex mechanisms further, providing new insights into the molecular processes underlying mutagenesis and dormancy.

Results and Discussion

The transient unculturability is largely driven by the global regulator RecA, crucial for the SOS response and recovery

To study UV-mediated mutagenesis and the SOS response, we used our previously established methodology[50]. We cultured *E. coli* MG1655 wild-type cells in 2 mL Lysogeny Broth (LB) medium in test tubes until they reached the mid-exponential phase with an optical density (OD_{600}) of ~0.5. Subsequently, the cells were transferred to petri dishes, forming a thin film of cultures that increased the surface area for UV exposure. This film was then subjected to UV-B light (302 nm thin-line transilluminator, UV intensity ~2000 μW/cm^2, UVP ChemStudio, Analytik Jena) for various durations: 2, 4, 8, 16, 24, and 32 minutes (min). Following exposure, the cells were promptly transferred back to test tubes and cultured in a shaker for 24-hour (h) recovery (refer to the Materials and Methods section for details). Cultures that did not receive UV-B treatment served as controls. During recovery, colony-forming units (CFU) were quantified at the indicated time points for each condition, as shown in **Fig. 1a**. At the beginning of recovery (t~0), CFU levels decreased in cultures exposed to longer UV-B treatments. A 4-8 min exposure caused a 10-fold reduction, while 16 min led to a ~100-fold drop compared to the control. Exposure times of 24 and 32 min resulted in a ~10,000-fold reduction (**Fig. 1a**). After 15 minutes, CFU levels notably increased in cultures with 24 and 32 min of UV-B exposure, likely due to mechanisms making cells temporarily unculturable. This drastic increase in CFU levels is not due to cell division, given that the *E. coli* doubling time is about 20-25 minutes, which is too short for significant growth within that period. By the 24-hour mark, all conditions showed similar CFU levels (**Fig. 1a**).

131 To measure mutagenesis, we quantified rifampicin (RIF)-resistant colonies after 24 hours of
132 recovery. Cultures were plated on LB agar with 500 μg/ml RIF, and colony counts were reported
133 per 10^8 cells (**Fig. 1b**). Although this method does not directly measure mutation levels, it is widely
134 used [40,51–53] due to the strong correlation between mutagenesis and resistant colony formation [54,55].
135 We chose a 24-hour recovery period to ensure accurate colony counts, consistent with previous
136 studies[51,56,57], as mutation levels generally plateau by this time[50]. Our results showed that
137 mutagenesis increased with UV-B exposure, peaking at 16 minutes, but longer exposures (24-32
138 min) significantly reduced RIF-resistant colonies (**Fig. 1b**). This pattern, consistent with our
139 previous findings[50], suggests a link between UV-B exposure, mutagenesis, and temporary
140 unculturability.

141 In our previous study, we found that excessive UV-B treatment (24 and 32 minutes) impaired the
142 SOS response, including the expression level of the RecA protein[50]. Therefore, the observed
143 transient unculturability is likely more complex and may involve various mechanisms, given that
144 the SOS response is intricate, involving multiple proteins, with RecA serving as the global
145 regulator. We hypothesized that if the observed transient unculturability is linked to the impaired
146 SOS response, then genetic perturbation of this response through *recA* deletion would further
147 decrease cell culturability. Our results verified that the knockout strain of *recA* exhibited a drastic
148 reduction in culturability immediately after UV treatment across all conditions (**Fig. 1c**). Initially,
149 CFU levels in the Δ*recA* strain were below the limit of detection (1 CFU) for most UV treatment
150 conditions; however, this was transient, as we observed a rapid increase in CFU levels (from 1 to
151 10^7) within 15 minutes of recovery (**Fig. 1c**). This finding is highly interesting and, to our
152 knowledge, has not been previously reported. As we have already shown the deletion *recA*
153 eliminates the mutagenesis following UV treatment[50], the impairment of the RecA-mediated SOS
154 response during prolonged UV exposures[50] should significantly affect downstream processes.
155 However, it remains unclear how these downstream processes impact cell culturability and
156 mutagenesis; thus, we aim to investigate these aspects in the subsequent sections of our study.

157 ***Genes significantly expressed during the SOS response have a moderate or negligible effect on***
158 ***cell culturability and mutagenesis***

159 To identify the downstream mechanisms, we screened a subset of the *E. coli* promoter library
160 containing 1900 promoter reporters. In this library, the promoters of *E. coli* genes are fused to a
161 fast-folding green fluorescent protein (GFP) gene in low-copy-number plasmids, allowing
162 accurate and reproducible measurement of gene expression[58]. We focused on approximately 40
163 reporters containing promoters that regulate the key SOS response and associated genes. These
164 promoters are under the control of the RecA-LexA regulatory system, chosen based on a
165 comprehensive analysis of *E. coli* databases[59]. In our experiments, *E. coli* MG1655 cells containing
166 the selected promoters were cultured individually until the mid-exponential phase in 96-well
167 plates. Subsequently, they were exposed to UV-B radiation for 16 min. This duration was chosen
168 as it induces maximum SOS upregulation and mutagenesis without drastically impacting cell
169 culturability (**Fig. 1a,b**). Also, 16-min UV treatments were used as positive controls for the
170 subsequent sections. GFP levels were measured after 24 h of recovery, allowing adequate time for
171 UV-induced promoters to express GFP. High cell densities ensured reliable GFP measurements,
172 given that we used a plate reader in this screening assay.

173 Our specific focus was on genes showing significant upregulation following UV treatment (**Fig.**
174 **2a**), as they likely play pivotal roles in the downstream mechanisms of RecA-mediated SOS
175 response. Several promoters showed drastic upregulation, including P_{recA} and P_{lexA} (promoters of

genes encoding SOS response global regulators), P_{recN} and P_{rmuC} (promoters of genes involved in DNA recombinational repair), P_{sulA} (promoter of a gene encoding cell division inhibitor), P_{polB} and P_{dinB} (promoters of genes encoding DNA polymerase enzymes), P_{ftsK} (promoter of a gene encoding essential cell division protein), P_{sbmC} (promoters of a gene encoding inhibitor of DNA gyrase-mediated DNA supercoiling), and P_{ybfE} (promoter of a *lexA*-regulated gene whose function is not well characterized)[60] (**Fig.2a**). To determine whether the genes associated with the identified promoters are involved in SOS response-mediated culturability and mutagenesis, we generated single deletions in *E. coli* MG1655 for these genes (except for *lexA* and *ftsK*, as they are essential and could not be deleted[61–63]). The knockout strains were exposed to UV-B for 16 min or 32 min or untreated, and their CFU profiles during recovery, as well as their RIF-resistant colony levels, were similarly measured. For all knockout strains, the temporal CFU profiles remained the same as that of the wild-type, showing a transient non-culturability during the first 15 min of recovery after a high UV-B exposure duration of 32 min (**Fig. 2b**). As expected, the deletion of *recA* completely eliminated mutagenesis (**Fig. 2c**). Although 32 min of UV-B exposure significantly reduced mutagenesis in all strains, including wild type, the two DNA recombination gene knockouts, Δ*recN* and Δ*rmuC*, showed a 3-fold and 1.5-fold decrease in RIF-resistant mutant levels, respectively, compared to WT cells following 16 min of UV-B treatment (**Fig. 2c**). Surprisingly, other single deletion strains, including those for the genes encoding DNA polymerase II and IV, *dinB* and *polB*, did not show significant changes (**Fig. 2c**).

Overall, our results showed that single deletions of the downstream genes of RecA did not drastically impact cellular culturability and mutagenesis, except for RecN and RmuC deletions, which slightly reduced mutagenesis. RecN is involved in the recombinational repair of DNA double-strand breaks, and its mutation makes cells sensitive to mitomycin C and ionizing radiation[64–66]. Although RmuC is thought to be an inner membrane protein with a nuclease domain[67,68], its function is not well understood, and our data indicate it only moderately impacts UV-B-mediated mutagenesis. It is quite surprising that the deletion of DNA polymerase II and IV, two key proteins involved in indirect mutagenesis[69], did not impact UV-B-induced mutagenesis. As mutagenesis is a multifaceted process regulated by multiple mechanisms, testing multi-deletion strains might be necessary to show the complex interplay between these mechanisms. Furthermore, deleting a single polymerase enzyme may have minimal impact due to the abundance of other polymerase enzymes. We first generated Δ*recN*Δ*rmuC* and showed that the double deletion resulted in a cumulative decrease (~5 fold) in RIF-resistant colony levels compared to the wild type following 16 min of UV-B treatment (**Fig. 2c**). To assess the impact of DNA polymerase II and IV, we generated a Δ*polB*Δ*dinB* mutant strain, which did not affect RIF-resistant colony levels (**Fig. 2c**). Additionally, we generated Δ*recN*Δ*polB* and Δ*recN*Δ*dinB* double knockout strains and demonstrated that they exhibited approximately a 5-fold reduction in RIF-resistant colony levels compared to wild-type cells (**Fig. 2c**). Deletion of DNA polymerase genes *polB* and *dinB* from Δ*recN*Δ*rmuC* individually did not show significant changes compared to the Δ*recN*Δ*rmuC* strain in RIF-resistant mutant levels (**Fig. 2c**), suggesting that the observed reduction in RIF-resistant colonies in multi-deletion strains is primarily due to the effects of *recN* and/or *rmuC*.

Screening the knockout strains reveals the redundancy of repair mechanisms in UV-induced mutagenesis and culturability

Although our initial screening yielded intriguing results, the critical downstream mechanisms underlying our observed phenomenon still remain elusive. Thus, we conducted a second screening using the *E. coli* BW25113 Keio knockout collection to assess the impact of UV on mutagenesis

221 and culturability of the knockout strains. This screening focused on all potential repair mechanisms
222 involved[12], particularly those (i) that are not regulated by RecA and (ii) whose expression was not
223 significantly upregulated in our initial screening (**Fig. 2a**). For this screening, the knockout strains
224 in 96-well plates were treated with UV-B for 16 min during mid-exponential-phase growth, and
225 RIF-resistant colonies were quantified after a 24-hour recovery period. We identified several genes
226 whose deletion resulted in a significant reduction in RIF-resistant colony formation (**Fig. 3a**),
227 including *recB*, a component of Exonuclease V or the RecBCD complex that promotes
228 homologous recombination in the repair of double-strand DNA breaks[70,71]; *umuC* and *umuD*,
229 encoding error-prone DNA polymerase V[72]; *ruvC*, encoding an endonuclease that binds to and
230 cleaves Holliday junctions[73]; and *katE*, encoding *E. coli* catalase enzyme[74]. Additionally, we
231 observed several genes that showed an increase in mutagenesis, such as *uvrD* and *uvrA*, which are
232 involved in the nucleotide excision repair pathway[75,76], and *mutY*, involved in the base excision
233 repair pathway[77] (**Fig. 3a**).

234 To better understand how these genes affect mutagenesis and culturability, and to see if similar
235 trends occur in other *E. coli* strains, we deleted these genes in *E. coli* MG1655 and analyzed the
236 knockout strains after 16 and 32 min of UV-B exposure. Deletion of *recB*, *ruvC*, *umuC*, and *umuD*
237 significantly reduced mutagenesis (**Fig. 3c**), consistent with our screening data. The absence of
238 UmuC and UmuD proteins, specialized for translesion synthesis, was shown to sensitize *E. coli*
239 cells to UV[78,79], aligning with our findings. While Δ*uvrA* in the *E. coli* BW25113 strain from
240 screening showed higher mutant levels compared to wild-type cells, its deletion in the MG1655
241 background resulted in a significant reduction in mutant formation (**Fig. 3c**), suggesting that the
242 role of certain genes in mutagenesis can vary depending on the genetic background of the *E. coli*
243 strain. Also, our results indicate that KatE, UvrD, and MutY may not be directly involved in the
244 mutagenic response to UV radiation under the conditions tested here, as their deletions did not
245 clearly impact UV-B-induced mutagenesis in *E. coli* MG1655 (**Fig. 3c**). Interestingly, Δ*uvrD* and
246 Δ*mutY* strains exhibited increased RIF-resistant colonies in cultures not treated with UV-B (**Fig.
247 3c**). UvrD is involved in various DNA repair pathways, including NER and MMR processes[37,80,81].
248 MutY is a glycosylase enzyme that corrects adenine mismatches resulting from DNA replication
249 errors, primarily in the BER pathway[77]. While the specific roles of UvrD and MutY in UV-B-
250 induced mutagenesis are not evident in this study, the increased RIF-resistant colonies in untreated
251 cultures might highlight their potential role in maintaining genomic stability under normal growth
252 conditions, possibly by mitigating spontaneous mutations.

253 The temporal CFU profiles revealed interesting trends as well. Δ*ruvC*, Δ*umuC*, and Δ*umuD* strains
254 showed no significant change in transient non-culturability immediately after UV-B treatment
255 compared to the wild type (**Fig. 3b**). However, Δ*recB* exhibited a notable decrease in CFU levels,
256 while Δ*uvrA* and Δ*uvrD* mutants showed even more drastic reductions following UV-B treatment
257 compared to the wild type (**Fig. 3c**). This reduction in CFU levels was transient, as their levels
258 increased approximately 10^7 -fold within 15 min of recovery. UvrA and UvrD together form key
259 components of the NER pathway[80]. UvrA forms a complex with UvrB to detect DNA lesions,
260 while UvrD functions as a helicase to unwind and remove damaged DNA segments[81,82]. As both
261 UvrA and UvrD are regulated by the RecA protein[28], it is not surprising that the deletion of *recA*
262 resulted in drastic reductions in CFU levels following UV treatment (**Fig. 1c**). Since RecA is
263 essential for inducing the SOS response, its absence means that many DNA repair genes, including
264 *uvrA* and *uvrD*, are not upregulated in response to UV-induced DNA damage.

265

266 ***Excessive UV exposure impairs cellular translation processes***

267 Although our results highlight specific SOS proteins involved in mutagenesis and cell culturability,
268 it remains unclear why excessive UV exposure impairs *recA* expression and, consequently, the
269 SOS response. This impairment could be due to the activation of cellular mechanisms, such as
270 growth arrest proteins, which may help limit excessive DNA damage and mutagenesis.
271 Additionally, the production of toxic molecules, such as reactive oxygen species, or the inhibition
272 of certain cellular functions, like translation, may also contribute to this effect. These
273 mechanisms—namely the involvement of growth arrest proteins, reactive oxygen species, or the
274 inhibition of translation—will be thoroughly explored in the subsequent section of our study.

275 Within the SOS response, two genes, *sulA* and *tisB*, play key roles in cell growth inhibition. The
276 *sulA* gene in *E. coli* encodes a cell-division inhibitor that temporarily halts the cell cycle during
277 the SOS response, preventing damaged DNA from prematurely segregating into daughter cells[83].
278 On the other hand, *tisB* encodes a toxin protein that reduces cellular ATP levels[46,84]. This protein
279 may also induce reversible dormancy by suppressing cell metabolism. To investigate the individual
280 and combined effects of these genes, we constructed knockout strains of *E. coli* MG1655 Δ*sulA*,
281 Δ*tisB*, and Δ*sulA*Δ*tisB*. Similarly, these strains, at the mid-exponential phase, were exposed to
282 varying durations of UV-B radiation followed by a 24-hour recovery period. *E. coli* MG1655 WT
283 cells were used as the control group for comparison. Deleting *sulA* and *tisB* individually did not
284 alter the trend of transient non-culturability observed in our experiments. Specifically, the CFU
285 profiles initially showed a significant decrease after prolonged UV-B exposure of 24 and 32 min,
286 followed by a sharp increase within the first 15 min of recovery, similar to the wild-type strain
287 (**Fig. 1a vs Fig. 4a-c**). However, CFU levels of Δ*sulA*Δ*tisB* immediately after 24 and 32 min of
288 UV-B exposure (corresponding to the t~0 point on the CFU plots) were nearly 10-fold higher
289 compared to those of the wild-type or single knockout strains (**Fig. 1a vs Fig. 4a-c**). We observed
290 approximately a 10-fold increase in CFU levels within the first 15 min of recovery in the double
291 knockout strain, although this increase was not as pronounced as in the control or single knockout
292 strains (**Fig. 4a-c**). While deleting both genes enhanced the culturability of cells following UV-B
293 treatment, the phenomenon observed in the wild-type strain was not completely eliminated in the
294 double knockout strain, highlighting the complexity of the underlying mechanisms. No distinct
295 profiles of RIF-resistant mutants were observed after 24 hours of recovery in either single or
296 double-knockout strains compared to the wild-type strain (**Fig. 1b vs Fig. 4d-f**), indicating that
297 these genes are not directly involved in mutagenesis, although they may affect cellular culturability
298 to some extent.

299 UV radiation has the potential to damage cellular membranes and compromise essential cellular
300 functions[15]. This damage can lead to increased membrane permeability, leakage of cellular
301 contents, and, ultimately, cell death[85,86]. Additionally, prolonged exposure to UV radiation can
302 trigger excessive production of reactive oxygen species (ROS) within cells[87–89]. ROS are highly
303 reactive molecules that can cause oxidative damage to cellular components such as DNA, proteins,
304 and lipids, impairing cellular functions. It is possible that the 24-minute and 32-minute UV-B
305 treatments studied here may not be severe enough to kill the bacterial cells completely, but they
306 are likely sufficient to hinder cell growth and mutagenic processes by disrupting vital metabolic
307 processes. To characterize cellular membrane permeability, cells treated with UV-B were
308 immediately collected and incubated with propidium iodide (PI), a fluorescent dye that enters cells
309 with compromised membranes. Flow cytometry data indicated no significant increase in
310 permeabilization following prolonged UV-B treatment (32 min) up to 1 hour of recovery (**Fig. 5a**),

311 compared to both untreated cells and moderately UV-treated cells (16 min), which did not
312 markedly reduce CFU levels. Furthermore, when UV-treated samples were subjected to Amplex
313 Red reagent (see Materials and Methods for details) to detect hydrogen peroxide (H_2O_2), a primary
314 reactive oxygen species, no significant changes were observed in the 32-minute UV-treated cells
315 compared to untreated or 16-minute UV-treated cells (**Fig. 5b**), indicating H_2O_2 may not be a key
316 player. In our previous study, we found that ROS significantly affects cell culturability only when
317 their concentrations are much higher than physiological levels, and their impact on cell
318 culturability was observed to be non-transient [50].

319 UV exposure is known to interfere with ribosomal function by inducing crosslinks in ribosomal
320 RNAs[90], which can inhibit overall translation processes and impair the expression of SOS response
321 genes. To assess the effects of UV treatments on cellular translation, we analyzed GFP expression
322 under the control of the *recA* promoter (P_{recA}) at the single-cell level using *E. coli* MG1655 cells
323 carrying the pUA66 P_{recA}-*gfp* plasmids. The cells were subjected to UV-B treatments for 16 min
324 and 32 min, and *recA* expression was measured using flow cytometry during the early recovery
325 phase (**Fig. 5c**). UV-B treatment should activate promoters of SOS response genes and induce
326 *recA* expression. As expected, the 16-min UV-B treatment resulted in significantly higher *recA*
327 expression compared to untreated cells (**Fig. 5c, e**). However, the 32-min UV-B exposure resulted
328 in more heterogeneous and lower *recA* expression compared to the 16-min UV-B exposure (**Fig.
329 5c, e**), potentially implying an impairment in the translational process. This difference between the
330 16- and 32-min treatments cannot be solely attributed to increased cell death following 32 min of
331 UV-B exposure. Despite the observed transient culturability in the prolonged UV-exposure
332 culture, CFU levels in both conditions are nearly similar after the brief transient period, around 15
333 minutes of recovery culture (see the 0.25-hour time point in **Fig. 1a**). To substantiate the hypothesis
334 regarding the impairment of the translational process, we employed a GFP-expressing plasmid
335 where the GFP gene is tightly regulated by an isopropyl β-D-1-thiogalactopyranoside (IPTG)-
336 inducible T5 promoter and a strong $LacI^q$ repressor[91]. Our rationale was that if excessive UV-B
337 treatment indeed impairs translational processes, the levels of GFP expression in cells treated with
338 32 min of UV-B should be lower compared to those in the no-UV control or 16-minute UV-treated
339 cells, despite the presence of the inducer. We supplemented cell cultures with 0.1 mM IPTG
340 immediately before UV-B treatments. As anticipated, the 32-min UV-B treatment resulted in a
341 lower level of GFP expression compared to the no-UV control or the 16-minute UV-B treatment
342 (**Fig. 5d, f**). However, the 16-min UV-B treatment exhibited the highest GFP expression levels
343 (**Fig. 5d, f**), suggesting that moderate UV treatment (16 min) enhances translational activity,
344 whereas excessive UV-B treatment (32 min) slightly inhibits it. This moderate inhibitory effect of
345 excessive UV-B treatment on cellular translation, including RecA expression, likely impacts
346 overall cellular processes and compromises the SOS response. This was further validated when we
347 measured the expression levels of *uvrD* and *uvrA*—two critical genes involved in mutagenesis and
348 culturability. Their expression levels were slightly reduced under 32 minutes of UV treatment
349 compared to 16 minutes (**Fig. 6a-d**).

350 Altogether, our findings suggest that while prolonged UV-B treatments may not directly impact
351 membrane integrity or ROS levels, the observed unculturability of the cells likely results from a
352 combined effect of multiple factors, including cell growth inhibitors, impaired translation
353 processes, and downstream repair pathways. The impairment of cellular processes such as
354 translation may hinder the SOS response, as evidenced by the decreased expression of RecA in
355 cells treated with 32 min of UV-B (**Fig. 5e**). This interpretation is further supported by our findings
356 with the Δ*recA* strain, which exhibited near-complete unculturability immediately after UV

357 treatments. The immediate reduction in CFU levels in the knockout strains (Δ*recA*, Δ*uvrA* and
358 Δ*uvrD*), as well as in the wild-type strain exposed to prolonged UV, highlights the importance of
359 the SOS response in the initial phases of DNA damage repair. The transient nature of CFU
360 reduction in all these mutants also suggests that *E. coli* possesses redundant or numerous repair
361 mechanisms[12] that can partially restore culturability even when certain DNA repair pathways are
362 disrupted.

363 Conclusions

364 In this study, we investigated the effects of UV-B treatments on *E. coli* mutagenesis and
365 culturability and provided important insights into bacterial survival mechanisms under stress.
366 Mutagenesis, measured by RIF-resistant colony formation, peaked at 16 min of UV-B exposure
367 but decreased with longer exposures (24 and 32 min). The longer UV-B exposures also led to a
368 significant decrease in CFU levels, but this phenomenon was observed to be a transient state, as
369 we saw a drastic jump in CFU levels after a short recovery period. We also explored the role of
370 key SOS response genes and demonstrated that knockout strains lacking *sulA* and *tisB* genes
371 exhibited similar patterns of transient non-culturability as wild-type cells, although double
372 knockouts exhibited higher initial CFU levels post-exposure, indicating a partial role in
373 culturability. Further investigation revealed that excessive UV exposure did not significantly affect
374 membrane permeability or reactive oxygen species (ROS) levels but moderately impaired
375 translation processes, as evidenced by reduced expression of SOS response genes like *recA* or
376 IPTG-inducible fluorescent proteins. This impaired translation likely contributed to the observed
377 reduction in mutagenesis and transient non-culturability following prolonged UV exposure, given
378 the significant impact of *recA* deletion on cell culturability and mutagenesis.

379 Although our screening of promoter reporters highlighted several genes significantly upregulated
380 following UV treatment, the knockout strains of most of these genes generally had minimal impact
381 on culturability or mutagenesis, except for Δ*recN* and Δ*rmuC*, which moderately reduced
382 mutagenesis. In our second screening with the Keio knockout collection, we identified several
383 critical genes, such as *recB, umuC, umuD*, and *ruvC*, whose deletions led to decreased
384 mutagenesis, highlighting their crucial roles in facilitating error-prone repair mechanisms during
385 UV-B stress. Furthermore, we observed differential impacts of gene deletions on mutagenesis
386 versus culturability, providing insights into additional functions of these genes. Particularly in
387 strains lacking *uvrA*, or *uvrD* showed a drastic but transient reduction in their culturability
388 following UV treatment, highlighting their role in maintaining genomic stability. Our findings also
389 underline the abundance of repair mechanisms in *E. coli*, demonstrating that multiple independent
390 pathways can significantly impact cell mutagenesis and culturability. Overall, this study
391 contributes to understanding bacterial responses to environmental stressors and the complex
392 interactions of DNA repair pathways in maintaining genomic integrity, culturability, and survival.

393 Materials and Methods

394 Bacterial strains and plasmids

395 *Escherichia coli* K-12 MG1655 wild type (WT), and pUA66 plasmids with genes encoding a green
396 fluorescent protein (*gfp*) under the control of promoter, P_{recA} were obtained from Dr. Mark P.
397 Brynildsen at Princeton University. *E. coli* K-12 MG1655 Δ*sulA,* Δ*tisB,* Δ*recA* was constructed in
398 our previous studies [50,92,93]. The promoter strain collection of *E. coli* MG1655 in a 96-well plate
399 format used for the screening assay was obtained from Horizon Discovery, Lafayette, CO, USA.
400 The Keio knockout strain collection (a single-gene deletion library of E. coli K-12 BW25113) was

401 obtained from Dharmacon Keio Collection (Dharmacon, Cat# OEC4988)**.** The strains from both
402 the collections used in this study are listed in **Supplementary Table 1**. The knockout *E. coli*
403 MG1655 strains generated for this study are detailed in **Supplementary Table 2**. The method of
404 Datsenko and Wanner[94] was used to generate these strains and the oligonucleotides used to delete
405 the genes are provided in **Supplementary Table 3.**

406 **Chemicals, media, and culture conditions**

407 Unless otherwise specified, all chemicals were procured from Fisher Scientific (Atlanta, GA),
408 VWR International (Pittsburgh, PA), or Sigma Aldrich (St. Louis, MO). PI staining kit was
409 purchased from Promega Corporation (Madison, WI). *E. coli* cells were cultured in liquid
410 Lysogeny-Broth (LB) medium. LB agar medium was utilized for enumerating colony-forming
411 units (CFU) of *E. coli*. The liquid LB medium was prepared by dissolving 5 g yeast extract, 10 g
412 tryptone, and 10 g sodium chloride in 1 L of deionized (DI) water. LB Agar media were prepared
413 by dissolving pre-mixed 40 g LB agar in 1 L of DI water. Both solid and liquid media were
414 subjected to autoclaving for sterilization.

415 Kanamycin (50 µg/mL) was included in the liquid LB media for plasmid selection and retention.
416 IPTG at 0.1 mM was used to induce *gfp* expression. For PI staining, sterile 0.85% sodium chloride
417 solution was used. When necessary, cells were washed with phosphate-buffered saline (PBS, 1X).
418 Stock solutions for rifampicin (RIF; 50 mg/mL) was prepared by dissolving in DI water using
419 0.01 N sodium hydroxide. The IPTG stock solution (1 mM) was dissolved in DI water. All
420 chemical solutions were sterilized using 0.2 µm VWR syringe filters.

421 To prepare RIF-agar plates, the stock RIF solution was added to autoclaved LB agar, resulting in
422 a final plate concentration of 500 µg/mL RIF. Unless specified otherwise, overnight pre-cultures
423 were generated in 14-mL Falcon test tubes containing 2 mL of liquid media. These pre-cultures
424 were inoculated from a 25% glycerol cell stocks stored at −80 °C and cultivated for 24 h at 37 °C
425 with shaking at 250 revolutions per min (rpm). Experimental cell cultures were prepared by
426 diluting the overnight pre-cultures (1:100) into 2 mL of fresh LB medium in 14-mL Falcon test
427 tubes. Bacterial cells in this study reached the mid-exponential phase ($OD_{600} \sim 0.5$) after around 3
428 h, attaining an average cell density of $7x10^8$ CFUs/ml. All treatments involving UV were
429 administered at this stage.

430 **UV treatment and cell recovery**

431 Overnight pre-cultures of *E. coli* MG1655 cells were diluted 100-fold in 2 mL fresh LB media in
432 test tubes and grown at 37°C with shaking (250 rpm). Cell growth was monitored by measuring
433 optical density at 600 nm wavelength (OD_{600}) with a plate reader (Varioskan LUX Multimode
434 Microplate Reader, Thermo Fisher, Waltham, MA, United States). When the cell density reached
435 $OD_{600} \sim 0.5$, cultures from the test tubes were transferred to petri dishes (the diameter of petri
436 dishes= 100 mm, catalog no. FB0875713, Fisher Scientific). This procedure created a thin film of
437 culture in the dish with a height of about 0.25 mm. Then, these cultures were exposed to a light
438 source emitting UV-B (302 nm) at approximately 2000µW (UVP ChemStudio, catalog no. 849-
439 97-0928-02; Analytik Jena, Jena, Germany) for varying exposure times (0, 2, 4, 8, 16, 24 and 32
440 min). After UV exposure, cells were transferred back to test tubes and recovered for 24 h. During
441 the recovery period, 10 µl samples were collected at specified time points from each test tube,
442 serially diluted in PBS in round-bottom 96-well plates, and then, plated on LB agar media. The
443 plates were incubated at 37 °C for 16 h to enumerate CFU. We note that new colonies were not
444 formed when incubated beyond 16 h. A similar procedure was followed for the other strains.

445 **Assessing mutagenesis**

446 To assess the extent of mutant cell formation induced by UV exposure, cells were exposed to UV
447 radiation for the specified durations, followed by a 24-h recovery period. After this recovery
448 period, 500 µL of cells were collected and spread onto agar plates containing 500 µg/mL of RIF.
449 These plates were then incubated at 37 °C for 16 h to enumerate RIF-resistant colonies. To
450 determine clonogenic survival, CFU levels were determined, and mutant levels were normalized
451 by dividing the number of RIF-resistant colonies by the total number of colonies in a 1 mL culture
452 volume. Unless specified otherwise, mutant formation was reported as the count of RIF-resistant
453 colonies per 10^8 cell population.

454 **PI Staining**

455 Mid-exponential *E. coli* cells were treated with UV for 16 min and 32 min duration following the
456 protocol mentioned above. At the beginning of the recovery and 1h after the recovery (t=0 h and
457 1 h), UV-treated cells in LB media were diluted 20-fold in 1.0 ml 0.85% NaCl solution in flow
458 cytometry tubes (5 ml round bottom Falcon tubes, size: 12 × 75 mm) to achieve the desired cell
459 density (~10^6-10^7 cells/ml) for flow cytometry analysis. The resulting cell suspensions were treated
460 with 20 µM PI dye. PI produces red fluorescence upon binding DNA; however, it can only
461 penetrate cells with damaged membranes. The samples were incubated in the dark at 37 °C for
462 15 min before analyzing them with a conventional bench-top flow cytometer (NovoCyte
463 3000RYB, ACEA Biosciences Inc., San Diego, CA, United States). For flow cytometry analysis,
464 we chose a slow sample flow rate (14 µl/ min) to have a sample stream diameter (i.e., core
465 diameter) of 7.7 µm. The instrument has a constant sheath flow rate of 6.5 ml/min. The flow
466 cytometer utilizes low-power solid-state lasers. Cells were excited at a 561 nm wavelength and red
467 fluorescence was detected with a 615/20-nm bandpass filter. At least 30,000 events were recorded
468 for each sample. NovoExpress software was used to collect the data. PI-stained dead cells, obtained
469 after ethanol (70% v/v) treatment, were used as a positive control. PI-stained live cells were used
470 as a negative control. Forward and side scatter signals of untreated live cells were used to
471 determine the cells on flow cytometry diagrams; the positive and negative controls were used to
472 gate PI positive (+) and PI negative (-) cell populations **(Supplementary Fig. S1)**

473 **H_2O_2 measurement**

474 The Amplex™ Red Hydrogen Peroxide/Peroxidase Assay Kit (Invitrogen, Thermo fischer
475 scientific, Catalog number: A22188) was used to assess the amount of H_2O_2 formed in the UV-
476 treated cells. The Amplex™ Red Hydrogen Peroxide/Peroxidase Assay Kit contains a sensitive,
477 one-step assay that uses the Amplex™ Red reagent (10-acetyl-3,7-dihydroxyphenoxazine) in
478 combination with horseradish peroxidase (HRP) to detect hydrogen peroxide (H_2O_2). In the
479 presence of peroxidase, the Amplex™ Red reagent reacts with H_2O_2 in a 1:1 stoichiometry to
480 produce the red-fluorescent oxidation product, resorufin. Resorufin has excitation and emission
481 maxima of approximately 571 nm and 585 nm. For preparing the stock solutions, 10 mM Amplex®
482 Red reagent was prepared by dissolving the contents of the vial of Amplex® Red reagent in 60 µL
483 of DMSO. Reaction buffer was diluted 5-fold to prepare 1X reaction buffer and 10 U/mL
484 Horseradish Peroxidase (HRP) was prepared by dissolving one vial of HRP in 1.0 mL of 1X
485 Reaction Buffer. The working solution of 100 µM Amplex® Red reagent and 0.2 U/mL HRP was
486 prepared by adding 50 µL of 10 mM Amplex® Red reagent stock solution and 100 µL of 10 U/mL
487 HRP stock solution in 4.85 mL of 1X Reaction Buffer. The assay volume for this experiment was

488 100 µL. Mid-exponential *E. coli* cells were treated with UV for 16 min and 32 min duration and
489 right after the treatment, 50 µL of sample for each condition was serially diluted in 1X Reaction
490 Buffer to determine the optimal amount of sample for the assay. 50 µL of the Amplex® Red
491 reagent/HRP working solution was added to each microplate well containing the samples. The
492 samples were incubated at room temperature for 30 min, and protected from light. At the end, the
493 fluorescence was measured using a microplate reader equipped for excitation in the range of 530–
494 560 nm and fluorescence emission detection at ~590 nm. For the standard curve, 20 mM Hydrogen
495 Peroxide (H_2O_2) working solution was prepared by dissolving 3.0% (0.88 M) H_2O_2 in 1X Reaction
496 Buffer and then further diluting 20 mM H_2O_2 working solution into 1X Reaction Buffer to produce
497 H_2O_2 concentrations of 0 to 10 µM, each in a volume of 50 µL. 50 µL of the Amplex® Red
498 reagent/HRP working solution was added to each microplate well containing the standards
499 followed by 30 min of incubation and then measuring the fluorescence following the same way
500 **(Supplementary Fig. S2).**

501 **Fluorescent protein expression assay for reporter genes**

502 Overnight pre-cultures of *E. coli* MG1655 cells with reporter genes fused to the SOS gene
503 promoters (P_{recA}, P_{uvrA}, and P_{uvrD}) were diluted 1:100 in 2 mL of LB media within test tubes and
504 incubated at 37°C with shaking (250 rpm). Upon reaching the mid-exponential phase, the cells
505 were subjected to UV radiation for specified durations (16 min and 32 min). An untreated culture
506 was used as a control. At the beginning of the recovery, 20 µM PI dye was added to the cultures
507 for continuous monitoring of the membrane permeability. At specified time points during the
508 recovery (t=0, 0.25, 0.5, 1, 2, 3 and 4 h), UV-treated cells were diluted 20-fold in 1.0 ml 0.85%
509 NaCl solution in flow cytometry tubes (5 ml round bottom Falcon tubes, size: 12 × 75 mm) to
510 achieve the desired cell density (~10^6-10^7 cells/ml). The samples were analyzed using the same
511 flow cytometry method described above (see the "PI staining" section); however, cells were
512 analyzed using two lasers. For measuring the red fluorescence from PI dye, cells were excited at a
513 561 nm wavelength, and red fluorescence was detected with a 615/20-nm bandpass filter. For
514 measuring the green fluorescence, cells were excited at a 488 nm wavelength, and the green
515 fluorescence was detected with a 530/30 bandpass filter.

516 **Transcription/translation activities of pUA66-*gfp* plasmid**

517 To assess the effect of the UV treatment on transcription/translation, the amount of GFP produced
518 by *E. coli* strains from the low-copy plasmid was measured. The plasmid, pUA66-*gfp*, has a *gfp*
519 gene under the control of a strong, IPTG-inducible T5 promoter and a strong $LacI^q$ repressor.
520 Overnight pre-cultures of *E. coli* MG1655 cells carrying pUA66-*gfp* were diluted 100-fold in 2
521 mL fresh LB media in test tubes and grown at 37°C with shaking (250 rpm). At the mid-
522 exponential phase (OD_{600}~0.5), 0.1mM IPTG was added to the test tubes and then immediately
523 treated with UV for 16 min and 32 min duration. Untreated cultures having IPTG only (without
524 UV exposure) served as controls. At specified time points during the recovery (t=0, 0.25, 0.5, 1,
525 2, 3, and 4 h), UV-treated cells were diluted 20-fold in 1.0 ml PBS in flow cytometry tubes (5 ml
526 round bottom Falcon tubes, size: 12 × 75 mm) to achieve the desired cell density (~10^6-10^7
527 cells/ml). The samples were analyzed using the same flow cytometry method described above (see
528 the "PI staining" section); however, cells were analyzed with a laser emitting light at 488 nm and
529 the green fluorescence was detected with a 530/30 bandpass filter.

530 **Promoter library screening**

531 Overnight precultures were prepared by inoculating the strains from the promoter library into the
532 wells of 96-well plates containing 200 µl LB medium and 50 µg/ml kanamycin (for plasmid
533 retention). The plates were sealed with a sterile, oxygen-permeable membrane (Breathe-Easier,
534 Cat# BERM-2000, VWR International) and cultured for 24 h at 37°C with shaking at 250 rpm.
535 Overnight precultures were diluted 1:40 in LB medium with kanamycin in a new 96-well plate,
536 sealed, and incubated at 37°C with shaking at 250 rpm. At the mid-exponential phase (OD_{600} =
537 0.5), cultures in 96 well plates were exposed to UV light (UVP ChemStudio, catalog no. 849-97-
538 0928-02; Analytik Jena, Jena, Germany) for 16 min, and then, recovered for 24 h at 37°C with
539 shaking at 250 rpm. GFP was measured with a Varioskan LUX Multimode Microplate Reader
540 (Thermo Fisher, Waltham, MA, USA) at the indicated times with untreated cultures as a control.
541 The excitation and emission wavelengths for GFP measurement were 485 nm and 511 nm,
542 respectively. Fold changes for GFP (treated/untreated cultures after 24 h treatment) were used to
543 report the promoter activity. The top 10 promoters showing the highest expression were selected
544 for subsequent experiments.

545 **Screening *E. coli* BW25113 Keio knockout collection**

546 Overnight cultures of single mutants **(Supplementary Table 1)** carrying kanamycin resistance
547 genes were diluted 40-fold into flat-bottom 96-well plates, with each well containing 200 µL of
548 cell culture. Kanamycin (50 µg/ml) was added to overnight and treatment cultures to prevent
549 contamination. The plates were securely sealed using a sterile, oxygen-permeable membrane
550 (Breathe-Easier, Cat# BERM-2000, VWR International) and incubated at 37°C with agitation at
551 250 rpm. When the cultures reached the mid-exponential phase (OD_{600} ~ 0.5), the cells in the 96-
552 well plates were exposed to UV light (UVP ChemStudio, catalog no. 849-97-0928-02; Analytik
553 Jena, Jena, Germany) for 16 min. Subsequently, they were allowed to recover for 24 h at 37°C
554 with shaking at 250 rpm. To quantify UV-induced mutant cells, 10 µL samples were collected
555 from each well and spotted onto LB agar plates, containing 500 µg/mL RIF, at the end of the 24-
556 h recovery period. The plates were then incubated at 37°C for 16 h to enumerate RIF-resistant
557 colonies. The mutant formation was reported as the count of RIF-resistant colonies per 10 µL of
558 cell culture.

559 **Statistical analysis and reproducibility**

560 For all pairwise comparisons, one-way ANOVA with Dunnett's post-test was utilized. A minimum
561 of four independent biological replicates (unless otherwise specified) were conducted for
562 experiments involving UV exposure. In all figures, data corresponding to each time point
563 represents the mean value ± standard deviation. Regarding statistical significance analysis, the
564 threshold values were set as follows: *$P < 0.05$, **$P < 0.01$, ***$P < 0.001$, and ****$P < 0.0001$. All
565 figures were created using GraphPad Prism 10.0.2, and the statistical analyses were carried out
566 using GraphPad Prism 10.0.2 statistical functions. FlowJo V 10.7.1 was used to analyze the data
567 obtained from flow cytometry.

568 ## Acknowledgment

569 The authors would like to thank the members of Orman Lab for their help. This study was
570 supported by NIH/NIAID R01-AI143643.

571

572 ## Contributions

573 S.G. and M.A.O. conceived and designed the study. S.G. performed the experiments. S.G. and
574 M.A.O. analyzed the data and wrote the paper.

575 ## Corresponding author

576 Correspondence to Mehmet A. Orman (morman@central.uh.edu)

577 ## Declaration of interests

578 The authors declare no competing interests.

579 ## Data availability

580 All data in this manuscript are available in either the main text or supplementary files. All raw data
581 have been deposited in the Figshare repository (doi.org/10.6084/m9.figshare.27701493.v1).

582

583 ## References

584 1. Hershberg, R. Mutation—The Engine of Evolution: Studying Mutation and Its Role in the
585 Evolution of Bacteria. *Cold Spring Harb Perspect Biol* **7**, (2015).
586 2. MacLean, R. C., Torres-Barceló, C. & Moxon, R. Evaluating evolutionary models of
587 stress-induced mutagenesis in bacteria. *Nature Reviews Genetics 2013 14:3* **14**, 221–227
588 (2013).
589 3. Zimmermann, A., Prieto-Vivas, J. E., Voordeckers, K., Bi, C. & Verstrepen, K. J.
590 Mutagenesis techniques for evolutionary engineering of microbes – exploiting CRISPR-
591 Cas, oligonucleotides, recombinases, and polymerases. *Trends Microbiol* (2024)
592 doi:10.1016/J.TIM.2024.02.006.
593 4. Sung, W., Ackerman, M. S., Miller, S. F., Doak, T. G. & Lynch, M. Drift-barrier
594 hypothesis and mutation-rate evolution. *Proc Natl Acad Sci U S A* **109**, 18488–18492
595 (2012).
596 5. Wielgoss, S. *et al.* Mutation rate dynamics in a bacterial population reflect tension
597 between adaptation and genetic load. *Proc Natl Acad Sci U S A* **110**, 222–227 (2013).
598 6. Fitzgerald, D. M., Hastings, P. J. & Rosenberg, S. M. Stress-Induced Mutagenesis:
599 Implications in Cancer and Drug Resistance. *Annu Rev Cancer Biol* **1**, 119 (2017).
600 7. Morreall, J. F., Petrova, L. & Doetsch, P. W. Transcriptional mutagenesis and its potential
601 roles in the etiology of cancer and bacterial antibiotic resistance. *J Cell Physiol* **228**, 2257
602 (2013).
603 8. Russo, M., Sogari, A. & Bardelli, A. Adaptive evolution: How bacteria and cancer cells
604 survive stressful conditions and drug treatment. *Cancer Discov* **11**, 1886–1895 (2021).
605 9. Lambert, G. *et al.* An analogy between the evolution of drug resistance in bacterial
606 communities and malignant tissues. *Nat Rev Cancer* **11**, 375 (2011).
607 10. Rothschild, L. J. The Influence of UV Radiation on Protistan Evolution. *Journal of*
608 *Eukaryotic Microbiology* **46**, 548–555 (1999).
609 11. Rozema, J. *et al.* The role of UV-B radiation in aquatic and terrestrial ecosystems—an
610 experimental and functional analysis of the evolution of UV-absorbing compounds. *J*
611 *Photochem Photobiol B* **66**, 2–12 (2002).

612 12. Rastogi, R. P., Richa, Kumar, A., Tyagi, M. B. & Sinha, R. P. Molecular Mechanisms of
613 Ultraviolet Radiation-Induced DNA Damage and Repair. *J Nucleic Acids* **2010**, 32 (2010).
614 13. Sinha, R. P. & Häder, D. P. UV-induced DNA damage and repair: a review.
615 *Photochemical & Photobiological Sciences 2002 1:4* **1**, 225–236 (2002).
616 14. Krishna, S., Maslov, S. & Sneppen, K. UV-Induced Mutagenesis in Escherichia coli SOS
617 Response: A Quantitative Model. *PLoS Comput Biol* **3**, e41 (2007).
618 15. Kciuk, M., Marciniak, B., Mojzych, M. & Kontek, R. Focus on UV-Induced DNA
619 Damage and Repair—Disease Relevance and Protective Strategies. *Int J Mol Sci* **21**, 1–33
620 (2020).
621 16. Gray, N. F. Ultraviolet Disinfection. *Microbiology of Waterborne Diseases:*
622 *Microbiological Aspects and Risks: Second Edition* 617–630 (2014) doi:10.1016/B978-0-
623 12-415846-7.00034-2.
624 17. Hessling, M., Haag, R., Sieber, N. & Vatter, P. The impact of far-UVC radiation (200-230
625 nm) on pathogens, cells, skin, and eyes - a collection and analysis of a hundred years of
626 data. *GMS Hyg Infect Control* **16**, Doc07 (2021).
627 18. Black, H. S. *et al.* Photocarcinogenesis: an overview. *J Photochem Photobiol B* **40**, 29–47
628 (1997).
629 19. Douki, T., Court, M., Sauvaigo, S., Odin, F. & Cadet, J. Formation of the main UV-
630 induced thymine dimeric lesions within isolated and cellular DNA as measured by high
631 performance liquid chromatography-tandem mass spectrometry. *J Biol Chem* **275**, 11678–
632 11685 (2000).
633 20. Rupert, C. S. Enzymatic Photoreactivation: Overview. *Basic Life Sci* **5 A**, 73–87 (1975).
634 21. Seawell, P. C. *et al.* den V gene of bacteriophage T4 determines a DNA glycosylase
635 specific for pyrimidine dimers in DNA. *J Virol* **35**, 790–796 (1980).
636 22. Van Houten, B. Nucleotide excision repair in Escherichia coli. *Microbiol Rev* **54**, 18–51
637 (1990).
638 23. Rupp, W. D. & Howard-flanders, P. Discontinuities in the DNA synthesized in an
639 Excision-defective strain of Escherichia coli following ultraviolet irradiation. *J Mol Biol*
640 **31**, 291–304 (1968).
641 24. Wendel, B. M., Hollingsworth, S., Courcelle, C. T. & Courcelle, J. UV-induced DNA
642 damage disrupts the coordination between replication initiation, elongation and
643 completion. *Genes to Cells* **26**, 94–108 (2021).
644 25. Majchrzak, M., Bowater, R. P., Staczek, P. & Parniewski, P. SOS Repair and DNA
645 Supercoiling Influence the Genetic Stability of DNA Triplet Repeats in Escherichia coli. *J*
646 *Mol Biol* **364**, 612–624 (2006).
647 26. Simmons, L. A., Foti, J. J., Cohen, S. E. & Walker, G. C. The SOS Regulatory Network.
648 *EcoSal Plus* **3**, (2008).
649 27. Little, J. W. & Mount, D. W. The SOS regulatory system of Escherichia coli. *Cell* **29**, 11–
650 22 (1982).
651 28. Maslowska, K. H., Makiela-Dzbenska, K. & Fijalkowska, I. J. The SOS system: A
652 complex and tightly regulated response to DNA damage. *Environ Mol Mutagen* **60**, 368–
653 384 (2019).
654 29. Walker, G. C. Mutagenesis and inducible responses to deoxyribonucleic acid damage in
655 Escherichia coli. *Microbiol Rev* **48**, 60–93 (1984).
656 30. Montelone, B. A. DNA Repair and Mutagenesis. Second Edition. By Errol C Friedberg,
657 Graham C Walker, Wolfram Siede, Richard D Wood, Roger A Schultz, and, Tom

Ellenberger. Washington (DC): ASM Press. $179.95. xxix + 1118 p + 11 pl; ill.; index. ISBN: 1-55581-319-4. 2006. . *https://doi.org/10.1086/509407* **81**, 273–273 (2015).

31. Martins-Pinheiro, M., Marques, R. C. P. & Menck, C. F. M. Genome analysis of DNA repair genes in the alpha proteobacterium Caulobacter crescentus. *BMC Microbiol* **7**, 17 (2007).
32. Kuzminov, A. Recombinational Repair of DNA Damage in Escherichia coli and Bacteriophage λ . *Microbiology and Molecular Biology Reviews* **63**, 751–813 (1999).
33. Burckhardt, S. E., Woodgate, R., Scheuermann, R. H. & Echols, H. UmuD mutagenesis protein of Escherichia coli: overproduction, purification, and cleavage by RecA. *Proceedings of the National Academy of Sciences* **85**, 1811–1815 (1988).
34. Woodgate, R., Rajagopalan, M., Lu, C. & Echols, H. UmuC mutagenesis protein of Escherichia coli: purification and interaction with UmuD and UmuD'. *Proceedings of the National Academy of Sciences* **86**, 7301–7305 (1989).
35. Kato, T. & Shinoura, Y. Isolation and characterization of mutants of Escherichia coli deficient in induction of mutations by ultraviolet light. *MGG Molecular & General Genetics* **156**, 121–131 (1977).
36. Wang, Z. Translesion synthesis by the UmuC family of DNA polymerases. *Mutation Research/DNA Repair* **486**, 59–70 (2001).
37. Liu, J. *et al.* MutL sliding clamps coordinate exonuclease-independent Escherichia coli mismatch repair. *Nat Commun* **10**, (2019).
38. Lin, T. *et al.* Contribution of the SOS response and the DNA repair systems to norfloxacin induced mutations in E. coli. *Mar Life Sci Technol* **5**, 538–550 (2023).
39. Shibai, A. *et al.* Mutation accumulation under UV radiation in Escherichia coli. *Scientific Reports 2017 7:1* **7**, 1–12 (2017).
40. Badran, A. H. & Liu, D. R. Development of potent in vivo mutagenesis plasmids with broad mutational spectra. *Nature Communications 2015 6:1* **6**, 1–10 (2015).
41. Tillich, U. M., Lehmann, S., Schulze, K., Dühring, U. & Frohme, M. The Optimal Mutagen Dosage to Induce Point-Mutations in Synechocystis sp. PCC6803 and Its Application to Promote Temperature Tolerance. *PLoS One* **7**, e49467 (2012).
42. Hashimoto, S. *et al.* Isolation of auxotrophic mutants of diploid industrial yeast strains after UV mutagenesis. *Appl Environ Microbiol* **71**, 312–319 (2005).
43. Hijnen, W. A. M., Beerendonk, E. F. & Medema, G. J. Inactivation credit of UV radiation for viruses, bacteria and protozoan (oo)cysts in water: A review. *Water Res* **40**, 3–22 (2006).
44. Reed, N. G. The History of Ultraviolet Germicidal Irradiation for Air Disinfection. *Public Health Reports* **125**, 15 (2010).
45. Bergkessel, M., Basta, D. W. & Newman, D. K. The physiology of growth arrest: uniting molecular and environmental microbiology. *Nat Rev Microbiol* **14**, 549 (2016).
46. Dörr, T., Vulić, M. & Lewis, K. Ciprofloxacin causes persister formation by inducing the TisB toxin in Escherichia coli. *PLoS Biol* **8**, 29–35 (2010).
47. Völzing, K. G. & Brynildsen, M. P. Stationary-phase persisters to ofloxacin sustain DNA damage and require repair systems only during recovery. *mBio* **6**, (2015).
48. Santos, A. L. *et al.* Effects of UV radiation on the lipids and proteins of bacteria studied by mid-infrared spectroscopy. *Environ Sci Technol* **47**, 6306–6315 (2013).
49. Wurtmann, E. J. & Wolin, S. L. RNA under attack: Cellular handling of RNA damage. *Crit Rev Biochem Mol Biol* **44**, 34 (2009).

704 50. Ghosh, S. & Orman, M. A. Exploring the links between SOS response, mutagenesis, and
705 resistance during the recovery period. *Antimicrob Agents Chemother* **68**, (2024).
706 51. Barrett, T. C., Mok, W. W. K., Murawski, A. M. & Brynildsen, M. P. Enhanced antibiotic
707 resistance development from fluoroquinolone persisters after a single exposure to
708 antibiotic. *Nature Communications 2019 10:1* **10**, 1–11 (2019).
709 52. Krašovec, R. *et al.* Mutation rate plasticity in rifampicin resistance depends on
710 Escherichia coli cell-cell interactions. *Nat Commun* **5**, (2014).
711 53. Reynolds, M. G. Compensatory evolution in rifampin-resistant Escherichia coli. *Genetics*
712 **156**, 1471 (2000).
713 54. Pope, C. F., O'Sullivan, D. M., McHugh, T. D. & Gillespie, S. H. A Practical Guide to
714 Measuring Mutation Rates in Antibiotic Resistance. *Antimicrob Agents Chemother* **52**,
715 1209 (2008).
716 55. Rosche, W. A. & Foster, P. L. Determining Mutation Rates in Bacterial Populations.
717 *Methods* **20**, 4 (2000).
718 56. Lagage, V., Chen, V. & Uphoff, S. Adaptation delay causes a burst of mutations in
719 bacteria responding to oxidative stress. *EMBO Rep* **24**, (2023).
720 57. Rodríguez-Rojas, A. *et al.* Non-lethal exposure to H2O2 boosts bacterial survival and
721 evolvability against oxidative stress. *PLoS Genet* **16**, e1008649 (2020).
722 58. Zaslaver, A. *et al.* A comprehensive library of fluorescent transcriptional reporters for
723 Escherichia coli. *Nat Methods* **3**, 623–628 (2006).
724 59. Keseler, I. M. *et al.* The EcoCyc database: reflecting new knowledge about Escherichia
725 coli K-12. *Nucleic Acids Res* **45**, D543–D550 (2017).
726 60. Fernández De Henestrosa, A. R. *et al.* Identification of additional genes belonging to the
727 LexA regulon in Escherichia coli. *Mol Microbiol* **35**, 1560–1572 (2000).
728 61. Goodall, E. C. A. *et al.* The Essential Genome of Escherichia coli K-12. *mBio* **9**, (2018).
729 62. Yu, X.-C., Weihe, E. K. & Margolin, W. Role of the C Terminus of FtsK in Escherichia
730 coli Chromosome Segregation. *J Bacteriol* **180**, 6424 (1998).
731 63. Wang, L. & Lutkenhaus, J. FtsK is an essential cell division protein that is localized to the
732 septum and induced as part of the SOS response. *Mol Microbiol* **29**, 731–740 (1998).
733 64. Meddows, T. R., Savory, A. P., Grove, J. I., Moore, T. & Lloyd, R. G. RecN protein and
734 transcription factor DksA combine to promote faithful recombinational repair of DNA
735 double-strand breaks. *Mol Microbiol* **57**, 97–110 (2005).
736 65. Picksley, S. M., Attfield, P. V. & Lloyd, R. G. Repair of DNA double-strand breaks in
737 Escherichia coli K12 requires a functional recN product. *Mol Gen Genet* **195**, 267–274
738 (1984).
739 66. Wang, T. C. & Smith, K. C. Different effects of recJ and recN mutations on the
740 postreplication repair of UV-damaged DNA in Escherichia coli K-12. *J Bacteriol* **170**,
741 2555–2559 (1988).
742 67. Kosinski, J., Feder, M. & Bujnicki, J. M. The PD-(D/E)XK superfamily revisited:
743 identification of new members among proteins involved in DNA metabolism and
744 functional predictions for domains of (hitherto) unknown function. *BMC Bioinformatics* **6**,
745 (2005).
746 68. Lomize, A. L., Lomize, M. A., Krolicki, S. R. & Pogozheva, I. D. Membranome: a
747 database for proteome-wide analysis of single-pass membrane proteins. *Nucleic Acids Res*
748 **45**, D250–D255 (2017).

749 69. Napolitano, R., Janel-Bintz, R., Wagner, J. & Fuchs, R. P. P. All three SOS-inducible
750 DNA polymerases (Pol II, Pol IV and Pol V) are involved in induced mutagenesis. *EMBO*
751 *J* **19**, 6259 (2000).
752 70. Hickson, I. D., Robson, C. N., Atkinson, K. E., Hutton, L. & Emmerson, P. T.
753 Reconstitution of RecBC DNase activity from purified Escherichia coli RecB and RecC
754 proteins. *J Biol Chem* **260**, 1224–9 (1985).
755 71. Payne-Dwyer, A. L., Syeda, A. H., Shepherd, J. W., Frame, L. & Leake, M. C. RecA and
756 RecB: probing complexes of DNA repair proteins with mitomycin C in live Escherichia
757 coli with single-molecule sensitivity. *J R Soc Interface* **19**, (2022).
758 72. Reuven, N. B., Arad, G., Maor-Shoshani, A. & Livneh, Z. The mutagenesis protein UmuC
759 is a DNA polymerase activated by UmuD', RecA, and SSB and is specialized for
760 translesion replication. *J Biol Chem* **274**, 31763–31766 (1999).
761 73. Takahagi, M., Iwasaki, H., Nakata, A. & Shinagawa, H. Molecular analysis of the
762 Escherichia coli ruvC gene, which encodes a Holliday junction-specific endonuclease. *J*
763 *Bacteriol* **173**, 5747–5753 (1991).
764 74. Loewen, P. C. Isolation of catalase-deficient Escherichia coli mutants and genetic
765 mapping of katE, a locus that affects catalase activity. *J Bacteriol* **157**, 622–626 (1984).
766 75. Epshtein, V. *et al.* UvrD facilitates DNA repair by pulling RNA polymerase backwards.
767 *Nature* **505**, 372–377 (2014).
768 76. Orren, D. K. & Sancar, A. The (A)BC excinuclease of Escherichia coli has only the UvrB
769 and UvrC subunits in the incision complex. *Proc Natl Acad Sci U S A* **86**, 5237–5241
770 (1989).
771 77. de Oliveira, A. H. S., da Silva, A. E., de Oliveira, I. M., Henriques, J. A. P. & Agnez-
772 Lima, L. F. MutY-glycosylase: An overview on mutagenesis and activities beyond the GO
773 system. *Mutation Research/Fundamental and Molecular Mechanisms of Mutagenesis* **769**,
774 119–131 (2014).
775 78. Shurtleff, B. W., Ollivierre, J. N., Tehrani, M., Walker, G. C. & Beuning, P. J. Steric Gate
776 Variants of UmuC Confer UV Hypersensitivity on Escherichia coli. *J Bacteriol* **191**, 4815
777 (2009).
778 79. Wang, T. chien V. & Smith, K. C. Role of the umuC gene in postreplication repair in UV-
779 irradiated Escherichia coli K-12 uvrB. *Mutation Research/DNA Repair Reports* **145**, 107–
780 112 (1985).
781 80. Moolenaar, G. F., Moorman, C. & Goosen, N. Role of the Escherichia coli Nucleotide
782 Excision Repair Proteins in DNA Replication. *J Bacteriol* **182**, 5706 (2000).
783 81. Orren, D., Selby, C., Hearst, J. & Sancar, A. Post-incision steps of nucleotide excision
784 repair in Escherichia coli. Disassembly of the UvrBC-DNA complex by helicase II and
785 DNA polymerase I. *J Biol Chem* **267**, 780–788 (1992).
786 82. Bertrand-Burggraf, E., Selby, C. P., Hearst, J. E. & Sancar, A. Identification of the
787 different intermediates in the interaction of (A)BC excinuclease with its substrates by
788 DNase I footprinting on two uniquely modified oligonucleotides. *J Mol Biol* **219**, 27–36
789 (1991).
790 83. Higashitani, A., Ishii, Y., Kato, Y. & Horiuchi, K. Functional dissection of a cell-division
791 inhibitor, SulA, of Escherichia coli and its negative regulation by Lon. *Molecular and*
792 *General Genetics* **254**, 351–357 (1997).
793 84. Unoson, C. & Wagner, E. G. H. A small SOS-induced toxin is targeted against the inner
794 membrane in Escherichia coli. *Mol Microbiol* **70**, 258–270 (2008).

795 85. McKenzie, K. *et al.* The effects of 405 nm light on bacterial membrane integrity
796 determined by salt and bile tolerance assays, leakage of UV-absorbing material and
797 SYTOX green labelling. *Microbiology (N Y)* **162**, 1680 (2016).
798 86. Yeo, S. K. & Liong, M. T. Effects and applications of sub-lethal ultrasound,
799 electroporation and UV radiations in bioprocessing. *Ann Microbiol* **63**, 813–824 (2013).
800 87. Cadet, J., Douki, T. & Ravanat, J. L. Oxidatively generated base damage to cellular DNA.
801 *Free Radic Biol Med* **49**, 9–21 (2010).
802 88. Winterbourn, C. C. Reconciling the chemistry and biology of reactive oxygen species.
803 *Nature Chemical Biology 2008 4:5* **4**, 278–286 (2008).
804 89. Schieber, M. & Chandel, N. S. ROS Function in Redox Signaling and Oxidative Stress.
805 *Curr Biol* **24**, R453 (2014).
806 90. Zwieb, C., Ross, A., Rinke, J., Meinke, M. & Brimacombe, R. Evidence for RNA-RNA
807 cross-link formation in Escherichia coli ribosomes. *Nucleic Acids Res* **5**, 2705 (1978).
808 91. Orman, M. A. & Brynildsen, M. P. Inhibition of stationary phase respiration impairs
809 persister formation in E. coli. *Nature Communications 2015 6:1* **6**, 1–13 (2015).
810 92. Mohiuddin, S. G., Nguyen, T. V. & Orman, M. A. Pleiotropic actions of phenothiazine
811 drugs are detrimental to Gram-negative bacterial persister cells. *Communications Biology*
812 *2022 5:1* **5**, 1–15 (2022).
813 93. Mohiuddin, S. G., Massahi, A. & Orman, M. A. lon Deletion Impairs Persister Cell
814 Resuscitation in Escherichia coli. *mBio* **13**, (2022).
815 94. Datsenko, K. A. & Wanner, B. L. One-step inactivation of chromosomal genes in
816 Escherichia coli K-12 using PCR products. *Proc Natl Acad Sci U S A* **97**, 6640 (2000).
817
818
819
820
821
822
823
824
825
826
827
828
829
830
831
832

Figures

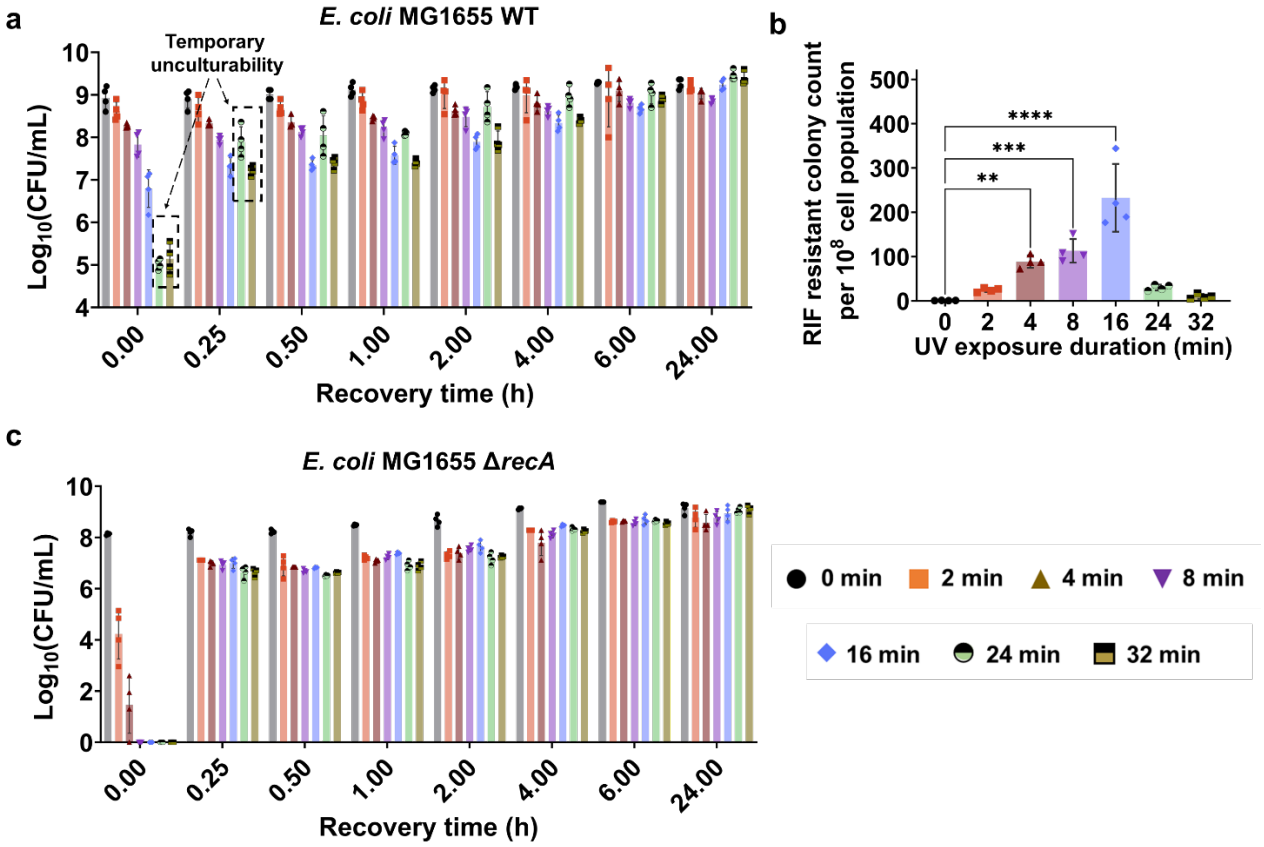

Fig. 1: Excessive UV exposure resulted in transient loss of culturability and decreased mutagenesis. (a) Exponential-phase *E. coli* MG1655 WT cells were exposed to UV-B light for 0, 2, 4, 8, 16, 24, and 32 minutes, followed by a 24-h recovery period. At specific time points during recovery (t = 0 h, 0.25 h, 0.5 h, 1 h, 2 h, 4 h, 6 h, and 24 h), cells were collected and plated to determine colony-forming units (CFU). (b) Levels of UV-induced rifampicin (RIF) resistance mutations were measured by counting RIF-resistant colonies (per 10^8 cells) in the WT cultures after recovery for the indicated UV exposure times. (c) The temporal CFU profiles of *E. coli* MG1655 Δ*recA* cells were monitored during recovery following UV treatment. n=4. Statistical analysis was performed using one-way ANOVA with Dunnett's post-test, where $*P < 0.05$, $**P < 0.001$, $***P < 0.01$, $****P < 0.0001$. Data corresponding to each time point represent mean value ± standard deviation.

853
854
855

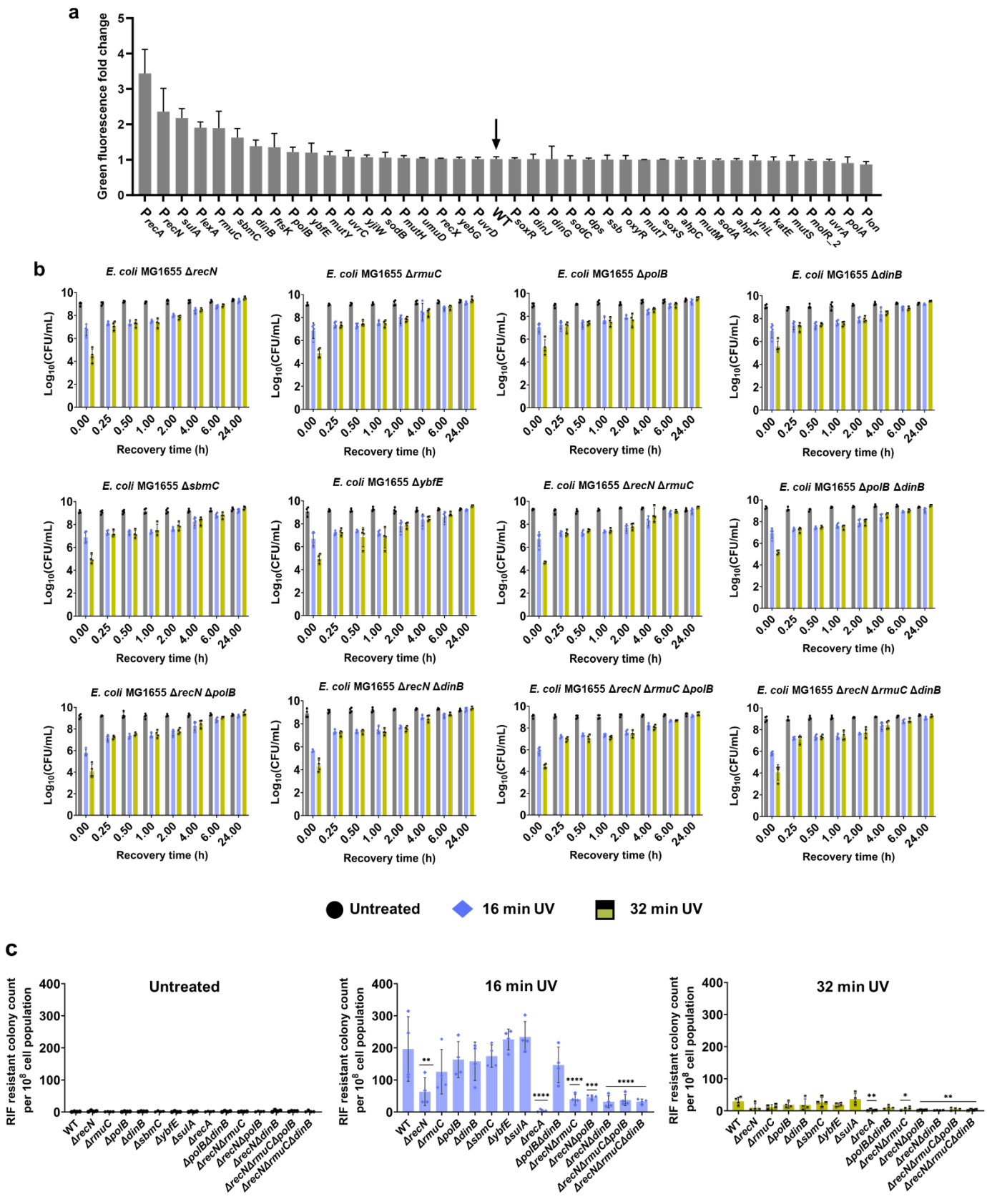
a
Green fluorescence fold change
P recA
P recN
P sulA
P lexA
P rmuC
P sbmC
P dinB
P ftsK
P polB
P ybfE
P mutY
P uvrC
P yjiW
P sodB
P mutH
P umuD
P recX
P yebG
P uvrD
WT
P soxR
P dinJ
P dinG
P sodC
P dps
P ssb
P oxyR
P mutT
P soxS
P ahpC
P mutM
P sodA
P ahpF
P yhiL
P katE
P mutS
P molR_2
P uvrA
P polA
P lon
b
E. coli MG1655 ΔrecN
E. coli MG1655 ΔrmuC
E. coli MG1655 ΔpolB
E. coli MG1655 ΔdinB
E. coli MG1655 ΔsbmC
E. coli MG1655 ΔybfE
E. coli MG1655 ΔrecN ΔrmuC
E. coli MG1655 ΔpolB ΔdinB
E. coli MG1655 ΔrecN ΔpolB
E. coli MG1655 ΔrecN ΔdinB
E. coli MG1655 ΔrecN ΔrmuC ΔpolB
E. coli MG1655 ΔrecN ΔrmuC ΔdinB
Log10(CFU/mL)
Recovery time (h)
0.00
0.25
0.50
1.00
2.00
4.00
6.00
24.00
Untreated
16 min UV
32 min UV
c
Untreated
16 min UV
32 min UV
RIF resistant colony count per 10^8 cell population
WT
ΔrecN
ΔrmuC
ΔpolB
ΔdinB
ΔsbmC
ΔybfE
ΔsulA
ΔrecA
ΔpolBΔdinB
ΔrecNΔrmuC
ΔrecNΔpolB
ΔrecNΔdinB
ΔrecNΔrmuCΔpolB
ΔrecNΔrmuCΔdinB

856

857 **Fig. 2: UV-induced upregulation of SOS genes and its impact on mutagenesis and cell**
858 **culturability.** (a) A library of *E. coli* MG1655 strains with promoter reporters for SOS response
859 genes was UV-treated during the mid-exponential phase and allowed to recover for 24 h. GFP
860 levels were measured after recovery and normalized to untreated controls. WT cells without any
861 promoter reporters were used as background controls. (b) Genes upregulated following UV
862 exposure were individually or combinatorially deleted in *E. coli* MG1655, and a mutagenesis assay
863 was performed. Mid-exponential phase cells were exposed to UV for 0, 16, and 32 min and
864 recovered for 24 h. At specified time points during recovery (t = 0 h, 0.25 h, 0.5 h, 1 h, 2 h, 4 h, 6
865 h, and 24 h), cells were collected and plated to determine CFU. (c) RIF-resistant cells were
866 quantified by plating samples on RIF-agar plates after 24 h of recovery, with results reported as
867 RIF-resistant colony counts per 10^8 cells for different UV exposure durations. n=4. Statistical
868 analysis was performed using one-way ANOVA with Dunnett's post-test, where $*P < 0.05$,
869 $**P < 0.001$, $***P < 0.01$, $****P < 0.0001$. Data corresponding to each time point represents mean
870 value ± standard deviation.
871
872
873
874
875
876
877
878
879
880
881
882
883
884
885
886
887
888
889
890
891
892
893
894
895

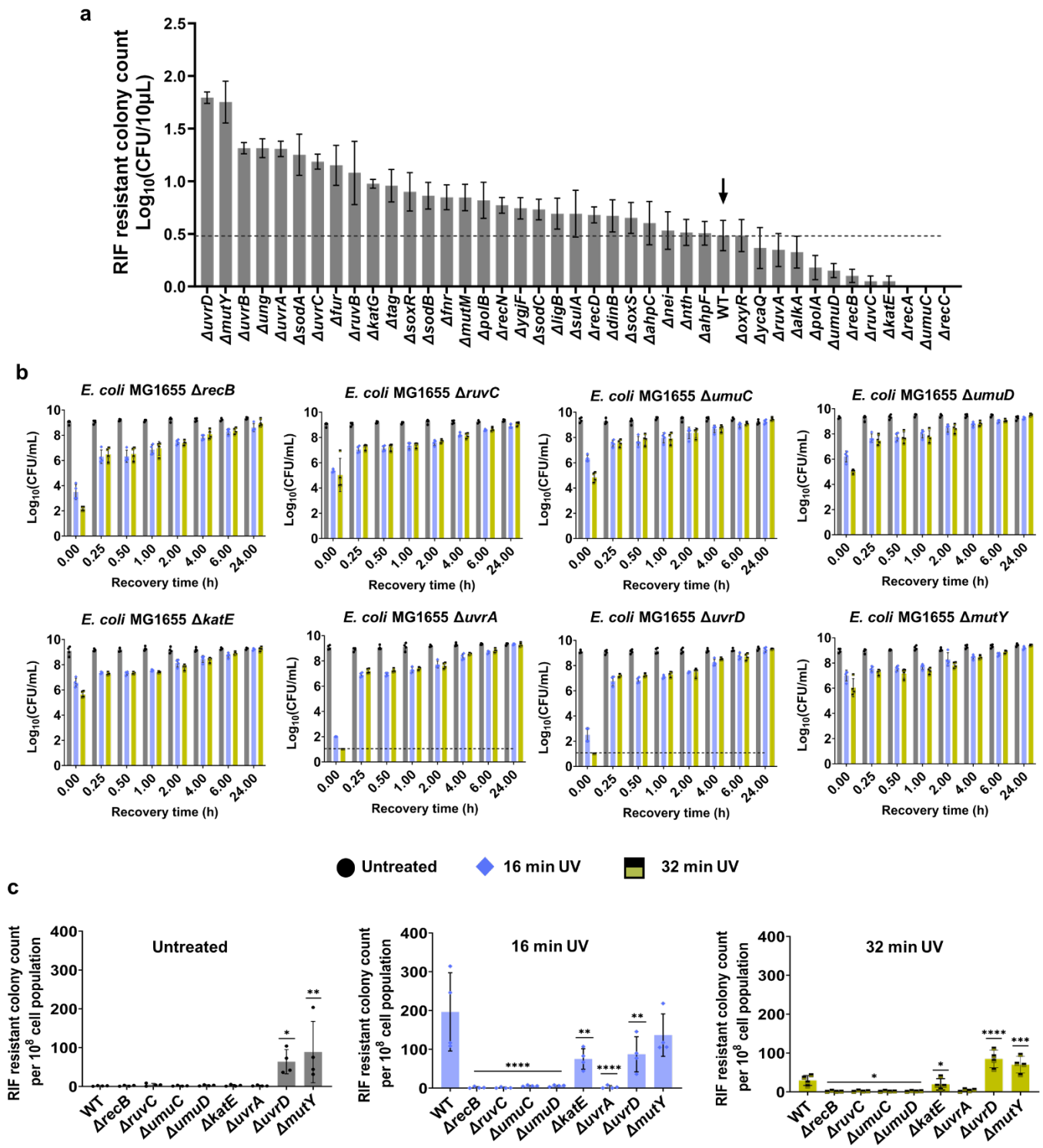

Fig. 3: Knockout library screening to elucidate their effects on mutagenesis and cell culturability. (a) The *E. coli* BW25113 Keio knockout collection was screened following 16 min of UV treatment. RIF-resistant cells were quantified by spotting 10 µL samples from each well onto RIF-agar plates after a 24-hour recovery period. (b) Selected genes were deleted in *E. coli* MG1655 and the mutagenesis assay was performed. Mid-exponential phase cells were exposed to

UV for 0, 16 and 32 min and recovered for 24 h. At indicated time points (t = 0 h, 0.25 h, 0.5 h, 1 h, 2 h, 4 h, 6 h and 24 h) during recovery, cells were collected and plated to enumerate CFU. (c) RIF-resistant cells were quantified by plating the samples on RIF-agar plates after 24 h of recovery. The values were reported as RIF-resistant colony count per 10^8 cell population for different UV exposure durations. n=4. Statistical analysis was performed using one-way ANOVA with Dunnett's post-test, where $*P < 0.05$, $**P < 0.001$, $***P < 0.01$. Data corresponding to each time point represents mean value ± standard deviation.

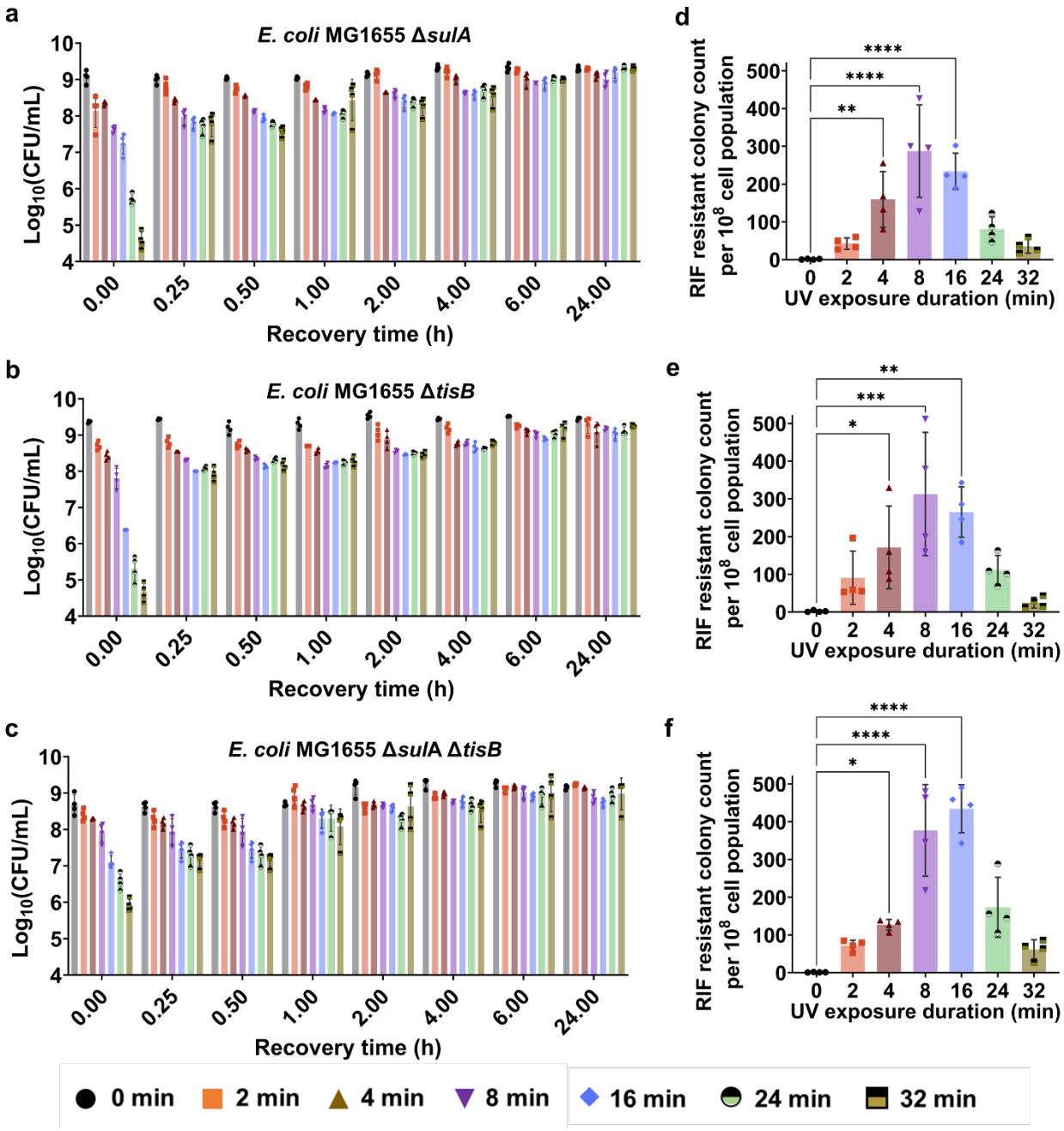

Fig. 4: Perturbation of both SulA and TiB proteins moderately increased cell culturability during recovery. (a-c) Exponential-phase *E. coli* MG1655 Δ*sulA*, Δ*tisB*, and Δ*sulA*Δ*tisB* cells were exposed to UV-B light for 0, 2, 4, 8, 16, 24, and 32 minutes, followed by a 24-h recovery period. At specific time points during recovery, cells were collected and plated to determine their CFU levels. (d-f) Levels of UV-induced RIF resistance mutations were measured by counting RIF-resistant colonies (per 10^8 cells) in the cultures of three knockout strains after recovery for the indicated UV exposure times. n=4. Statistical analysis was performed using one-way ANOVA with Dunnett's post-test, where $*P<0.05$, $**P<0.001$, $***P<0.01$, $****P<0.0001$. Data corresponding to each time point represent mean value ± standard deviation.

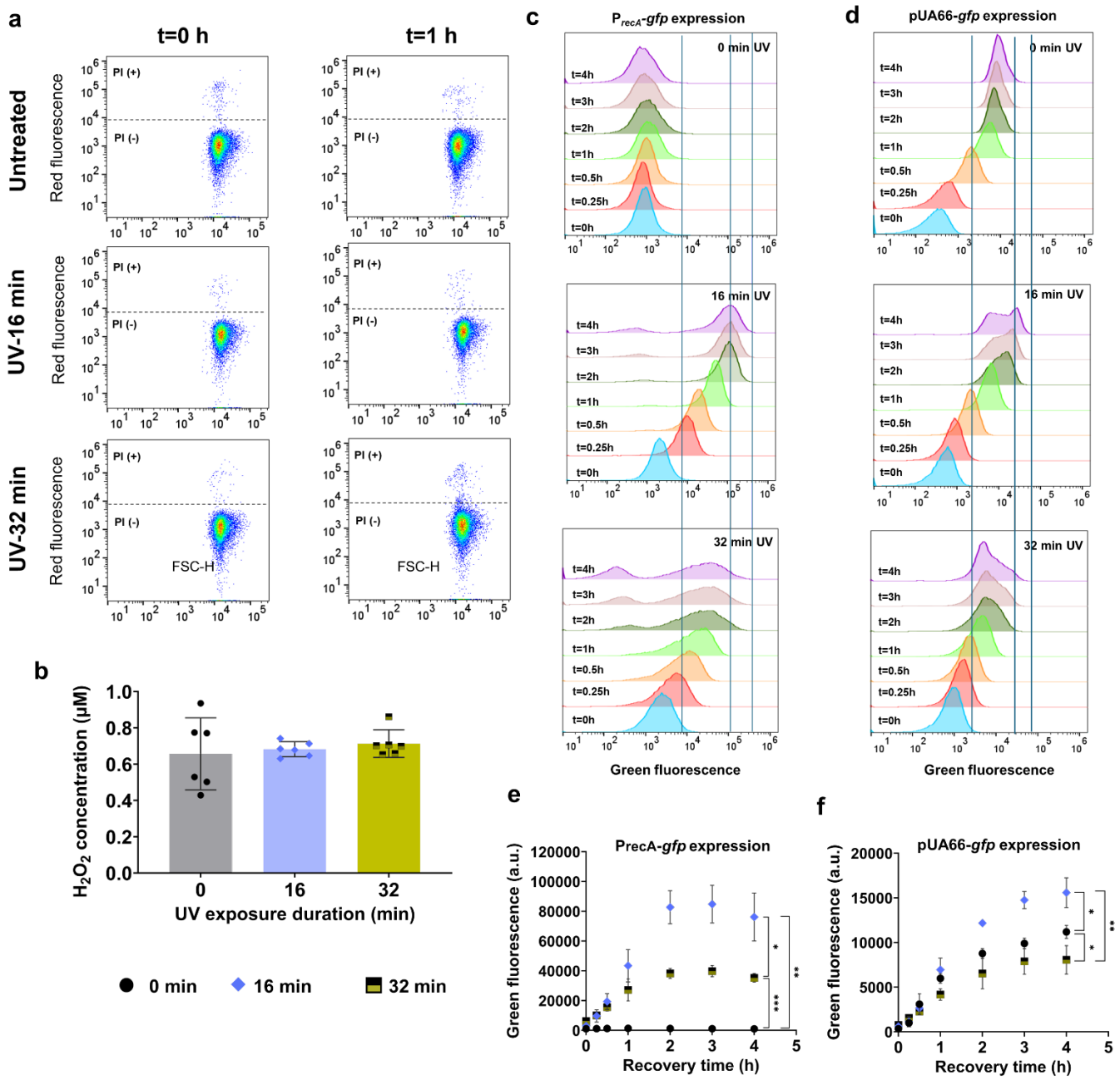

Fig. 5: Excessive UV exposure did not compromise cell membrane integrity or increase hydrogen peroxide levels, but it did impair cellular translation. (a) Membrane integrity of UV-treated cells (0, 16, and 32 min of UV exposure) was assessed via flow cytometry with PI staining (see **Supplementary Fig. S1** for controls). FSC-H: Forward light scatter. (b) H_2O_2 concentrations were measured using the Amplex Red Hydrogen Peroxide/Peroxidase Assay Kit. Reaction mixtures containing Amplex Red reagent, horseradish peroxidase, and UV-treated cells in sodium phosphate buffer (pH 7.4) were incubated for 30 minutes at room temperature, followed by fluorescence measurement with a microplate reader. H_2O_2 levels were calculated using a standard curve (**Supplementary Fig. S2**). (c) Expression of P_{recA}-*gfp* in UV-treated *E. coli* MG1655 cells was analyzed via flow cytometry for the indicated time points during recovery (P_{recA} : the *recA* promoter). (d) IPTG-inducible GFP expression in UV-treated *E. coli* MG1655 pUA66-*gfp* cells

was also assessed by flow cytometry for the indicated time points during recovery. (e) GFP expression profiles of UV-treated cells harboring the *recA* promoter and (f) IPTG-inducible GFP expression systems were evaluated using mean GFP values from flow cytometry data. Note that the vertical lines in the flow diagrams roughly represent the upper, lower, and peak fluorescence levels of the overall cell population exposed to the 16-min UV-B treatment (corresponding to the 4-h treatment time point). These lines were included to help readers more easily distinguish the outcomes of different experimental conditions. $n \geq 4$. Statistical analysis was performed using one-way ANOVA with Dunnett's post-test, where $*P < 0.05$, $**P < 0.001$, $***P < 0.01$, $****P < 0.0001$. Data corresponding to each time point represent mean value ± standard deviation.

997

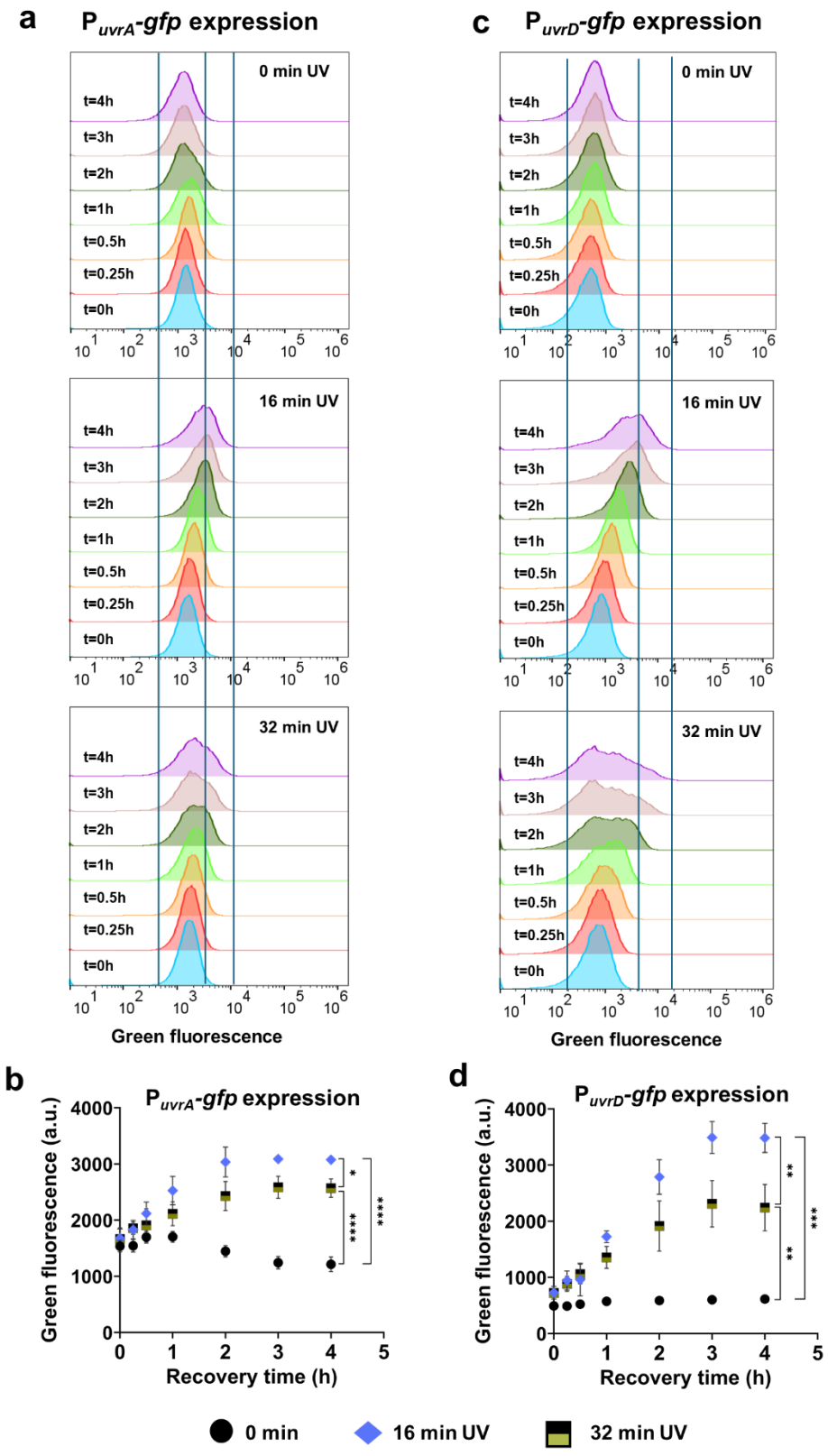
a
P uvrA-gfp expression
0 min UV
16 min UV
32 min UV
t=4h
t=3h
t=2h
t=1h
t=0.5h
t=0.25h
t=0h
Green fluorescence
c
P uvrD-gfp expression
b
P uvrA-gfp expression
Green fluorescence (a.u.)
Recovery time (h)
d
P uvrD-gfp expression
0 min
16 min UV
32 min UV

998

Fig. 6: Flow cytometry analysis of nucleotide excision repair genes followed by UV-treatment (a, b) The GFP profiles of UV-treated cells harboring P_{uvrA}-*gfp*, and (c, d) the GFP profiles of UV-treated cells harboring P_{uvrD}-*gfp* were assessed using flow cytometry after UV exposure (for the indicated time points during recovery). Note that the vertical lines in the flow diagrams roughly represent the upper, lower, and peak fluorescence levels of the overall cell population exposed to the 16-min UV-B treatment (corresponding to the 4-h treatment time point). These lines were included to help readers more easily distinguish the outcomes of different experimental conditions. n=4. Statistical analysis was performed using two-way ANOVA, where $*P < 0.05$, $**P < 0.001$, $***P < 0.01$, $****P < 0.0001$. Data corresponding to each time point represent mean value ± standard deviation.

Supplementary Information

UV-Induced DNA Repair Mechanisms and Their Effects on Mutagenesis and Culturability in *Escherichia coli*

Sreyashi Ghosh[1], and Mehmet A. Orman[1]*

[1]William A. Brookshire Department of Chemical and Biomolecular Engineering, University of Houston, Houston, TX, USA

*Correspondence to: S222 Engineering Bldg 1, 4226 Martin Luther King Boulevard, Houston, TX 77204-4004, Phone: 713-743-6785, Email: morman@central.uh.edu

Supplementary figures

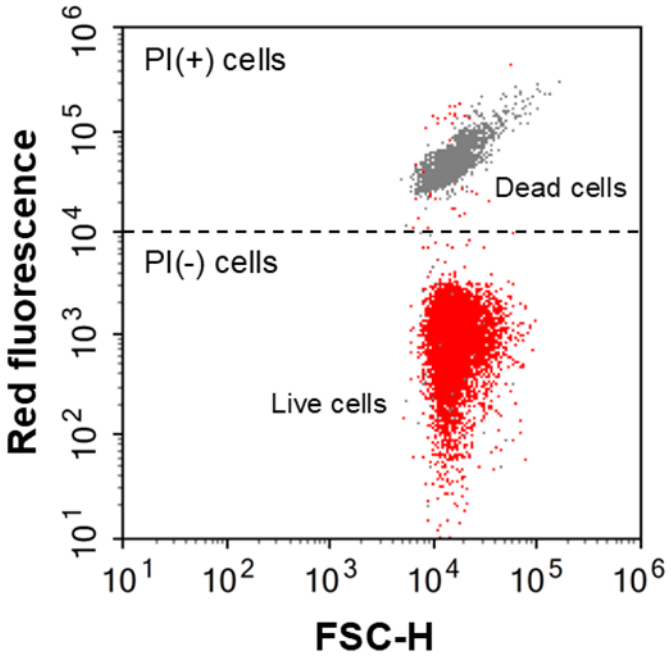

Fig. S1. PI staining of live and dead cells. Live cells (Red) and ethanol-treated dead cells (70% v/v, Grey) were stained with PI and analyzed by flow cytometry to assess live and dead cell populations. The figure shows a representative flow cytometry diagram. Similar results were observed across all independent biological replicates, n=4.

1053

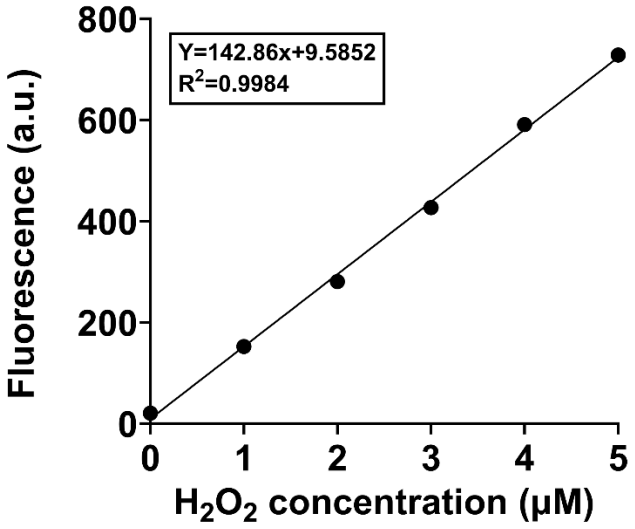

1054
1055
1056 **Fig. S2. Standard curve for H_2O_2 measurement using the Amplex Red Hydrogen**
1057 **Peroxide/Peroxidase Assay Kit.** The standard curve was generated using a 20 mM Hydrogen
1058 Peroxide (H_2O_2) working solution, prepared by dissolving 3.0% (0.88 M) H_2O_2 in 1X Reaction
1059 Buffer. This solution was then diluted in 1X Reaction Buffer to achieve H_2O_2 concentrations
1060 ranging from 0 to 10 μM, in 50 μL aliquots. To each microplate well containing the standards, 50
1061 μL of Amplex® Red reagent/HRP working solution was added. After a 30-minute incubation,
1062 fluorescence was measured using a microplate reader with excitation in the range of 530–560 nm
1063 and emission detection at ~590 nm.
1064

1065 **Supplementary tables**

1066

1067 **Table S1: Promoter library and single-deletion knockout library used in this study.**

Bacterial Strains	Source
E. coli K-12 MG1655 *pMSs201* P_{uvrA}-*gfp*	Promoter library from Horizon Discovery, Lafayette, CO, USA
E. coli K-12 MG1655 *pMSs201* P_{dps}-*gfp*	
E. coli K-12 MG1655 *pMSs201* P_{soxS}-*gfp*	
E. coli K-12 MG1655 *pMSs201* P_{recX}-*gfp*	
E. coli K-12 MG1655 *pMSs201* P_{molR}-*gfp*	
E. coli K-12 MG1655 *pMSs201* P_{polA}-*gfp*	
E. coli K-12 MG1655 *pMSs201* P_{dinG}-*gfp*	
E. coli K-12 MG1655 *pMSs201* P_{mutS}-*gfp*	
E. coli K-12 MG1655 *pMSs201* P_{mutH}-*gfp*	
E. coli K-12 MG1655 *pMSs201* P_{mutY}-*gfp*	
E. coli K-12 MG1655 *pMSs201* P_{ybfE}-*gfp*	
E. coli K-12 MG1655 *pMSs201* P_{sbmC}-*gfp*	
E. coli K-12 MG1655 *pMSs201* P_{mutM}-*gfp*	
E. coli K-12 MG1655 *pMSs201* P_{yjiW}-*gfp*	
E. coli K-12 MG1655 *pMSs201* P_{mutT}-*gfp*	
E. coli K-12 MG1655 *pMSs201* P_{dinB}-*gfp*	
E. coli K-12 MG1655 *pMSs201* P_{ftsK}-*gfp*	
E. coli K-12 MG1655 *pMSs201* P_{sodB}-*gfp*	
E. coli K-12 MG1655 *pMSs201* P_{recN}-*gfp*	
E. coli K-12 MG1655 *pMSs201* P_{rmuC}-*gfp*	
E. coli K-12 MG1655 *pMSs201* P_{dinJ}-*gfp*	
E. coli K-12 MG1655 *pMSs201* P_{yebG}-*gfp*	
E. coli K-12 MG1655 *pMSs201* P_{sulA}-*gfp*	
E. coli K-12 MG1655 *pMSs201* P_{soxR}-*gfp*	
E. coli K-12 MG1655 *pMSs201* P_{ahpC}-*gfp*	
E. coli K-12 MG1655 *pMSs201* P_{katE}-*gfp*	
E. coli K-12 MG1655 *pMSs201* P_{sodC}-*gfp*	
E. coli K-12 MG1655 *pMSs201* P_{ahpF}-*gfp*	
E. coli K-12 MG1655 *pMSs201* P_{yhiL}-*gfp*	
E. coli K-12 MG1655 *pMSs201* P_{uvrC}-*gfp*	
E. coli K-12 MG1655 *pMSs201* P_{oxyR}-*gfp*	
E. coli K-12 MG1655 *pMSs201* P_{polB}-*gfp*	
E. coli K-12 MG1655 *pMSs201* P_{uvrD}-*gfp*	
E. coli K-12 MG1655 *pMSs201* P_{sodA}-*gfp*	
E. coli K-12 MG1655 *pMSs201* P_{lexA}-*gfp*	
E. coli K-12 MG1655 *pMSs201* P_{recA}-*gfp*	

E. coli K-12 MG1655 *pMSs201* P_{lon}-*gfp*	
E. coli K-12 MG1655 *pMSs201* P_{umuD}-*gfp*	
E. coli K-12 MG1655 *pMSs201* P_{ssb}-*gfp*	
E. coli K-12 BW25113 Δ*fnr*	Keio collection, Cat# OEC4987
E. coli K-12 BW25113 Δ*soxR*	
E. coli K-12 BW25113 Δ*soxS*	
E. coli K-12 BW25113 Δ*umuD*	
E. coli K-12 BW25113 Δ*recA*	
E. coli K-12 BW25113 Δ*ruvB*	
E. coli K-12 BW25113 Δ*uvrD*	
E. coli K-12 BW25113 Δ*sodB*	
E. coli K-12 BW25113 Δ*sodC*	
E. coli K-12 BW25113 Δ*ahpF*	
E. coli K-12 BW25113 Δ*katG*	
E. coli K-12 BW25113 Δ*sodA*	
E. coli K-12 BW25113 Δ*ygjF*	
E. coli K-12 BW25113 Δ*polA*	
E. coli K-12 BW25113 Δ*ruvA*	
E. coli K-12 BW25113 Δ*ruvC*	
E. coli K-12 BW25113 Δ*umuC*	
E. coli K-12 BW25113 Δ*uvrA*	
E. coli K-12 BW25113 Δ*alkA*	
E. coli K-12 BW25113 Δ*ahpC*	
E. coli K-12 BW25113 Δ*sulA*	
E. coli K-12 BW25113 Δ*katE*	
E. coli K-12 BW25113 Δ*uvrB*	
E. coli K-12 BW25113 Δ*nei*	
E. coli K-12 BW25113 Δ*dinB*	
E. coli K-12 BW25113 Δ*recB*	
E. coli K-12 BW25113 Δ*nth*	
E. coli K-12 BW25113 Δ*uvrC*	
E. coli K-12 BW25113 Δ*fur*	
E. coli K-12 BW25113 Δ*ligB*	
E. coli K-12 BW25113 Δ*ung*	
E. coli K-12 BW25113 Δ*tag*	
E. coli K-12 BW25113 Δ*recN*	
E. coli K-12 BW25113 Δ*mutY*	
E. coli K-12 BW25113 Δ*ycaQ*	
E. coli K-12 BW25113 Δ*mutM*	

E. coli K-12 BW25113 Δ*recC*	
E. coli K-12 BW25113 Δ*polB*	
E. coli K-12 BW25113 Δ*recD*	
E. coli K-12 BW25113 Δ*oxyR*	
E. coli K-12 BW25113 Wild type	

1068
1069
1070 **Table S2: Bacterial plasmid and strains used in this study.**

Bacterial Strains	Source
E. coli K-12 MG1655 pUA66 P*recA-gfp*	Gift from Dr. Mark P. Brynildsen
E. coli K-12 MG1655 pUA66-*gfp*	Gift from Dr. Mark P. Brynildsen
E. coli K-12 MG1655 Wild type	Gift from Dr. Mark P. Brynildsen
E. coli K-12 MG1655 Δ*sulA*	Previous study
E. coli K-12 MG1655 Δ*tisB*	Previous study
E. coli K-12 MG1655 Δ*recA*	Previous study
E. coli K-12 MG1655 Δ*sulA*Δ*tisB*	This study
E. coli K-12 MG1655 Δ*recN*	This study
E. coli K-12 MG1655 Δ*rmuC*	This study
E. coli K-12 MG1655 Δ*polB*	This study
E. coli K-12 MG1655 Δ*dinB*	This study
E. coli K-12 MG1655 Δ*sbmC*	This study
E. coli K-12 MG1655 Δ*ybfE*	This study
E. coli K-12 MG1655 Δ*polB*Δ*dinB*	This study
E. coli K-12 MG1655 Δ*recN*Δ*rmuC*	This study
E. coli K-12 MG1655 Δ*recN*Δ*polB*	This study
E. coli K-12 MG1655 Δ*recN*Δ*dinB*	This study
E. coli K-12 MG1655 Δ*recN*Δ*rmuC*Δ*polB*	This study
E. coli K-12 MG1655 Δ*recN*Δ*rmuC*Δ*dinB*	This study
E. coli K-12 MG1655 Δ*recB*	This study
E. coli K-12 MG1655 Δ*ruvC*	This study
E. coli K-12 MG1655 Δ*umuC*	This study
E. coli K-12 MG1655 Δ*umuD*	This study
E. coli K-12 MG1655 Δ*katE*	This study
E. coli K-12 MG1655 Δ*uvrA*	This study
E. coli K-12 MG1655 Δ*uvrD*	Previous study
E. coli K-12 MG1655 Δ*mutY*	This study

1071
1072

1073 **Table S3: Oligonucleotides used the generating single and multi-deletion mutants**

Oligonucleotides to generate gene deletions			
Mutation	**Forward Primer (5' to 3'):**	**Reverse Primer (5' to 3')**	**Source**
Δ*recN*::KAN^R	ACACAATAACAGTAATGGTTTTTCATACAGGAAAACGACTGTGTAGGCTGGAGCTGCTTC	CGTTTTGCTGTTTACTCTGACCGTGAAGCAGGAAAAAAGTTTAACGGCTGACATGGGAAT	Integrated DNA Technologies, Inc.
Δ*rmuC*::KAN^R	CAGGAAATGCCTTTCCAACTGGACGTTTGTACAGCACAATTCTATTTTGTGCGGGTAAGTTGTTGCGTCAGGAGGCGTTGTGTAGGCTGGAGCTGCTTC	TCAAAAAATTGTTCCAGAAGTGTAACAGATTGGGCGTCGATGCCCTAGATTTCTACCCGGCTTAACTACTCCCAATGGGTTAACGGCTGACATGGGAAT	Integrated DNA Technologies, Inc.
Δ*polB*::KAN^R	CAGGCTATACTCAAGCCTGGTTTTTTGATGGATTTTCAGCGTGTAGGCTGGAGCTGCTTC	TCACGCATCAAAATGGTATCTGGCGAACTCTTTTTTTGCTTAACGGCTGACATGGGAAT	Integrated DNA Technologies, Inc.
Δ*dinB*::KAN^R	ACGCGTTAAATGCTGAATCTTTACGCATTTCTCAAACCCTGAAATCACTGTATACTTTA CCAGTGTTGAGAGGTGAGCA GTGTAGGCTGGAGCTGCTTC	CCGATTTTTCAGCGAGAATTCGATGCATACAGTGATACCCTCATAATAATGCACACCAGAATATACATAATAGTATACATTAACGGCTGACATGGGAAT	Integrated DNA Technologies, Inc.
Δ*sbmC*::KAN^R	CAACTATACTGTATATAAAAACAGTATCAATGGAGGCGTCGTGTAGGCTGGAGCTGCTTC	AAAGAGTGGTCATCGCGTTAACACACCGCCCTGAGATGAATTAACGGCTGACATGGGAAT	Integrated DNA Technologies, Inc.
Δ*ybfE*::KAN^R	AGAGGCCTGGCTGATTGTTTCCCCCGAAGTCACCAAGATCGTGTAGGCTGGAGCTGCTTC	ACGAGCAGGACTGCACACTGTGCTACATGAAAGTGGAAATTTAACGGCTGACATGGGAAT	Integrated DNA Technologies, Inc.
Δ*recB*::KAN^R	AGCGCGTTGCAGCAAACAATGCCCCTGATGAGTGAAAAGAGTGTAGGCTGGAGCTGCTTC	GCGGGCGTAGCTGTTTGTGCTCCACAGCTTCCAGTAATTGCTTTTGCAATTTCATTAACGGCTGACATGGGAAT	Integrated DNA Technologies, Inc.
Δ*ruvC*::KAN^R	CTCTGATGAGGCCTGCTAAACAGCAAAACGGAGACGCGTGGTGTAGGCTGGAGCTGCTTC	GTGGAAACGCCTCAGCCGGAACTGACCGAGGCGGTATAACTTA	Integrated DNA Technologies, Inc.

			ACGGCTGACATGGGAAT		
Δ*umuC*::KAN^R	TCTTTGGTGTGGTGATCCACGTCGTTAAGGCGATGCGCTGGTGTAGGCTGGAGCTGCTTC		TCGGCGCTCCTGCGGGAGCGCTTTTTTCCTGCCGCTATATTTAACGGCTGACATGGGAAT		Integrated DNA Technologies, Inc.
Δ*umuD*::KAN^R	GAACAGACTACTGTATATAAAAACAGTATAACTTCAGGCAGATTATTGTGTAGGCTGGAGCTGCTTC		CAGCTGGCATAAAACGCGTTTACATCACAGAGGGCAAACATTTAACGGCTGACATGGGAAT		Integrated DNA Technologies, Inc.
Δ*katE*::KAN^R	ACAGCGGCCCTTTCAGTAATAAATTAAGGAGACGAGTTCAGTGTAGGCTGGAGCTGCTTC		ATGTAAATCATTTGAGGCGGCGCAATTGCGCCGCCTCCCATTAACGGCTGACATGGGAAT		Integrated DNA Technologies, Inc.
Δ*uvrA*::KAN^R	ATGCCACCGGGCAAAAAAGCGTTTAATCCGGGAAAGGTGAGTGTAGGCTGGAGCTGCTTC		CTCTGAAAGGAAAAGGCCGCTCAGAAAGCGGCCTTAACGATTAACGGCTGACATGGGAAT		Integrated DNA Technologies, Inc.
Δ*mutY*::KAN^R	TGCTGCAATCTTGCCCCCAACAACAGTGAATTCGGTGACCGTGTAGGCTGGAGCTGCTTC		TCGTTCTGCTCATAAATCATCCTCTTTATCGACTCACGCGTTAACGGCTGACATGGGAAT		Integrated DNA Technologies, Inc.
Oligonucleotides to verify gene deletions					
Mutation	**External Forward Primer (5' to 3')**	**External Reverse Primer (5' to 3')**	**Internal Forward Primer (5' to 3')**	**Internal Reverse Primer (5' to 3')**	**Source**
Δ*recN*::KAN^R	GATTCGTCGCTGTGATTACCATC	GCTCTTCGTCCAGATCATCCT	GCACAACTGACCATCAGCAA	CAGTTGCTGCTGTTCTTCCAGTAG	Integrated DNA Technologies, Inc.
Δ*rmuC*::KAN^R	AAAGCCATGCGGTGAAAATC	GCTCTTCGTCCAGATCATCCT	GTTATTGCGTTGGTGGGTGT	GGGTTCAACGGGAATAAACA	Integrated DNA Technologies, Inc.
Δ*polB*::KAN^R	GTCAGTTAGCGCCGCAGTTA	GCTCTTCGTCCAGATCATCCT	GCGCAGGCAGGTTTTATCTT	GGTTTATCTTCGGCGAAACG	Integrated DNA Technologies, Inc.
Δ*dinB*::KAN^R	GACCAAAAGTGCGTCCGATA	GCTCTTCGTCCAGATCATCCT	GTGGATATGGACTGCTTTTTCG	GGCGTTCATCCCAGGTTTTA	Integrated DNA Technologies, Inc.

Δ*sbmC*::KAN^R	GGTTACCCTGGAATCTGTCG	GCTCTTCGTCCAGATCATCCT	GAAGAGAAACGTACCGTTGCAG	GCTGCACCGCAACATACATT	Integrated DNA Technologies, Inc.
Δ*ybfE*::KAN^R	TACGCGCTATCCGTCGCTAT	GCTCTTCGTCCAGATCATCCT	AACAAACGGACCGTACGACA	GCCAGTTGCTGCATTAACATCT	Integrated DNA Technologies, Inc.
Δ*recB*::KAN^R	TTCTTCCATCAGGCGGTGGT	GCTCTTCGTCCAGATCATCCT	ATCCACTGTACGAACGCCTG	AAATTCGGTACTGCTGGGGG	Integrated DNA Technologies, Inc.
Δ*ruvC*::KAN^R	GAAACCGCACCGAAACTGAT	GCTCTTCGTCCAGATCATCCT	GGCTATTATTCTCGGCATTGATCC	AACGTGGCAGTGGGTGATAG	Integrated DNA Technologies, Inc.
Δ*umuC*::KAN^R	CTGTTGACGGCGAGTTTACG	GCTCTTCGTCCAGATCATCCT	AGCTGTGAGACGGTGTTTCG	GATCGCGTAGCAGCGTTAAT	Integrated DNA Technologies, Inc.
Δ*umuD*::KAN^R	TTTTCATTTCTGCTGGATGAGC	GCTCTTCGTCCAGATCATCCT	TCTTGTTCAGTGTGGCTTTCC	TGGATCACCACACCAAAGACA	Integrated DNA Technologies, Inc.
Δ*katE*::KAN^R	GTTTAGCCGATTTAGCCCCTG	GCTCTTCGTCCAGATCATCCT	ATCAGCCGCTCACGGTTATT	TATGGTAAGGGCAGGTCGGA	Integrated DNA Technologies, Inc.
Δ*uvrA*::KAN^R	F_Ex_sodA: CACAACACTCCGGGTAATGC	GCTCTTCGTCCAGATCATCCT	TGAATCCCTTTCCGCCTACG	ACGGATGACGACGAATGGAG	Integrated DNA Technologies, Inc.
Δ*mutY*::KAN^R	CAAATTCCGGTGAAATGACG	GCTCTTCGTCCAGATCATCCT	GCCCAGGTTCTGGACTGGTA	CGACACGGGAAGCCACATAG	Integrated DNA Technologies, Inc.